Journal of Sedimentary Research

Journal of Sedimentary Research, 2023, v. 93, 552–570
Research Article
DOI: 10.2110/jsr.2022.104

MULTIPROXY PROVENANCE ANALYSES IN THE DEVONIAN VILLAVICENCIO FORMATION OF THE MENDOZA PRECORDILLERA, ARGENTINA: CORRELATION AND GEOTECTONIC IMPLICATIONS FOR THE SW GONDWANA MARGIN

FEDERICO D. WENGER,*[1] JONATAN A. ARNOL,[1] NORBERTO J. URIZ,[1] CARLOS A. CINGOLANI,[1,2] PAULINA ABRE,[3] AND MIGUEL A.S. BASEI[4]

[1]*División Científica de Geología–Facultad de Ciencias Naturales y Museo, Universidad Nacional de La Plata, Paseo del Bosque s/n, 1900 La Plata, Argentina*
[2]*Centro de Investigaciones Geológicas, Facultad de Ciencias Naturales y Museo, Universidad Nacional de La Plata, diag. 113 no. 275, La Plata, Argentina*
[3]*Geología y Recursos Minerales, Centro Universitario Regional Este, Universidad de la República, Treinta y Tres, Uruguay*
[4]*Instituto de Geociencias, Centro de Pesquisas Geocronológicas, Universidade de São Paulo, Brazil*
e-mail: wnm091@usask.ca

ABSTRACT: **This work focuses on the sedimentary provenance of the Villavicencio Formation of the Mendoza Precordillera and integrates the information obtained with previous work on other coeval units of the Precordillera Central of San Juan province (Gualilán Group: Talacasto and Punta Negra formations) in western Argentina. Multiproxy provenance analyses are carried out from different applied methodologies (petrography, geochemistry, morphological, and cathodoluminescence studies of detrital zircon grains, and analysis of U-Pb and Lu-Hf isotopes). The Villavicencio Formation is mostly composed of pelites and very fine-grained psammites. The major components are quartz, both monocrystalline and polycrystalline, and metamorphic lithics that associate this unit with a recycled orogen. Regarding geochemistry, the Chemical Index of Alteration (CIA) values are similar to the Post-Archean Australian Shales (PAAS), indicating a null to incipient degree of weathering. The ratios between different trace elements and rare earth elements (REEs) suggest the felsic composition of the source area. Th/U ratios differ, but a secondary uranium enrichment is inferred. The morphological analysis of the zircon grains reveals their mainly plutonic origin. The integration of U-Pb data with Lu-Hf data shows a juvenile-mantle origin in which the populations are dominantly Mesoproterozoic and εHf of positive values (up to 12), indicating poor differentiation. The Villavicencio Formation would be the product of deltaic deposits in which its components are dominantly from the Western Pampean Sierras associated with the Grenville orogen, assuming exhumation and erosion of the Mesoproterozoic basement. The data support the hypothesis of equivalence and correlation with the Punta Negra Formation in the Devonian depocenters of the south-central region of the San Juan Precordillera.**

INTRODUCTION

The lower Paleozoic sequences of western Argentina (28–33° S), especially the Cambrian–Ordovician, have been extensively studied (Waisfeld et al. 2023) to determine and understand the stages of paleogeographic evolution between the autochthonous margin of Gondwana (Fig. 1A) and the approach of the Cuyania Terrane (Fig. 1B). However, there are few studies on middle Paleozoic basin development along the western Gondwana margin at these latitudes. The first provenance approaches were made by Loske (1992, 1994, 1995) and Kury (1993, 1994) and more recently, the works based strictly on sedimentary provenance from units of the San Juan Precordillera (Abre et al. 2012; Arnol et al. 2020, 2022, 2023; Arnol and Coturel 2022) and the San Rafael Block (Manassero et al. 2009; Abre et al. 2011, 2017; Cingolani et al. 2017). In the Mendoza Precordillera (Fig. 1C), the Devonian sequence identified as Villavicencio Formation, is widely exposed (Fig. 2). Cingolani et al. (2013) provided the first U-Pb ages in detrital zircon indicating strong contributions of Mesoproterozoic ages (1400–1000 Ma) coincident with the two domains established by Rapela et al. (2016) for the Western Sierras Pampeanas (1030–1330 Ma).

The present work focuses on establishing the main patterns of sediment contribution that allow us to elucidate the paleogeographic and paleorelief features and their influence on the filling of the Villavicencio Devonian depocenter and its correlation with equivalent records in the San Juan Precordillera. The data obtained from petrography, geochemistry, morphological and cathodoluminescence studies of detrital zircon grains, and Lu-Hf isotope analysis have been integrated with the information collected in previous works for this region. Finally, the schematic paleogeography and tectonic setting in which the Devonian basin of the southwestern margin of Gondwana developed is discussed.

*Present Address: Department of Geological Sciences, University of Saskatchewan, Saskatoon, Saskatchewan S7N 5E2, Canada

Published Online: August 2023
 1527-1404/23/093-552

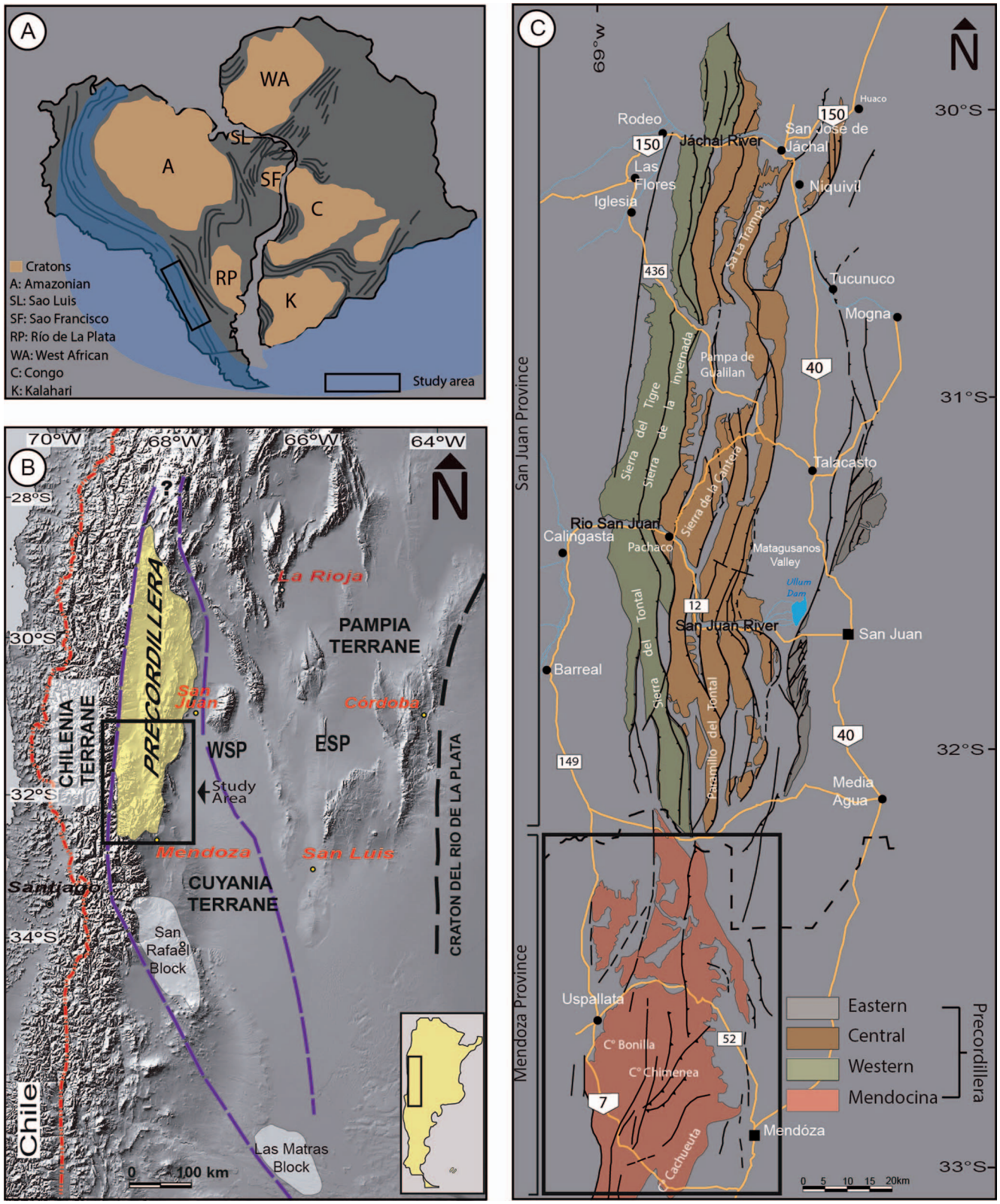

FIG. 1.—**A)** West Gondwana with cratons and study area. **B)** Extension of the Precordillera as part of Cuyania terrane. **C)** Tectonic subdivisions of the Precordillera in: Eastern, Central, Western in the San Juan Province, Mendoza Precordillera and La Rioja Precordillera in the homonymous provinces (modified from Ortiz and Zambrano 1981; Astini 1992; Ragona et al. 1995).

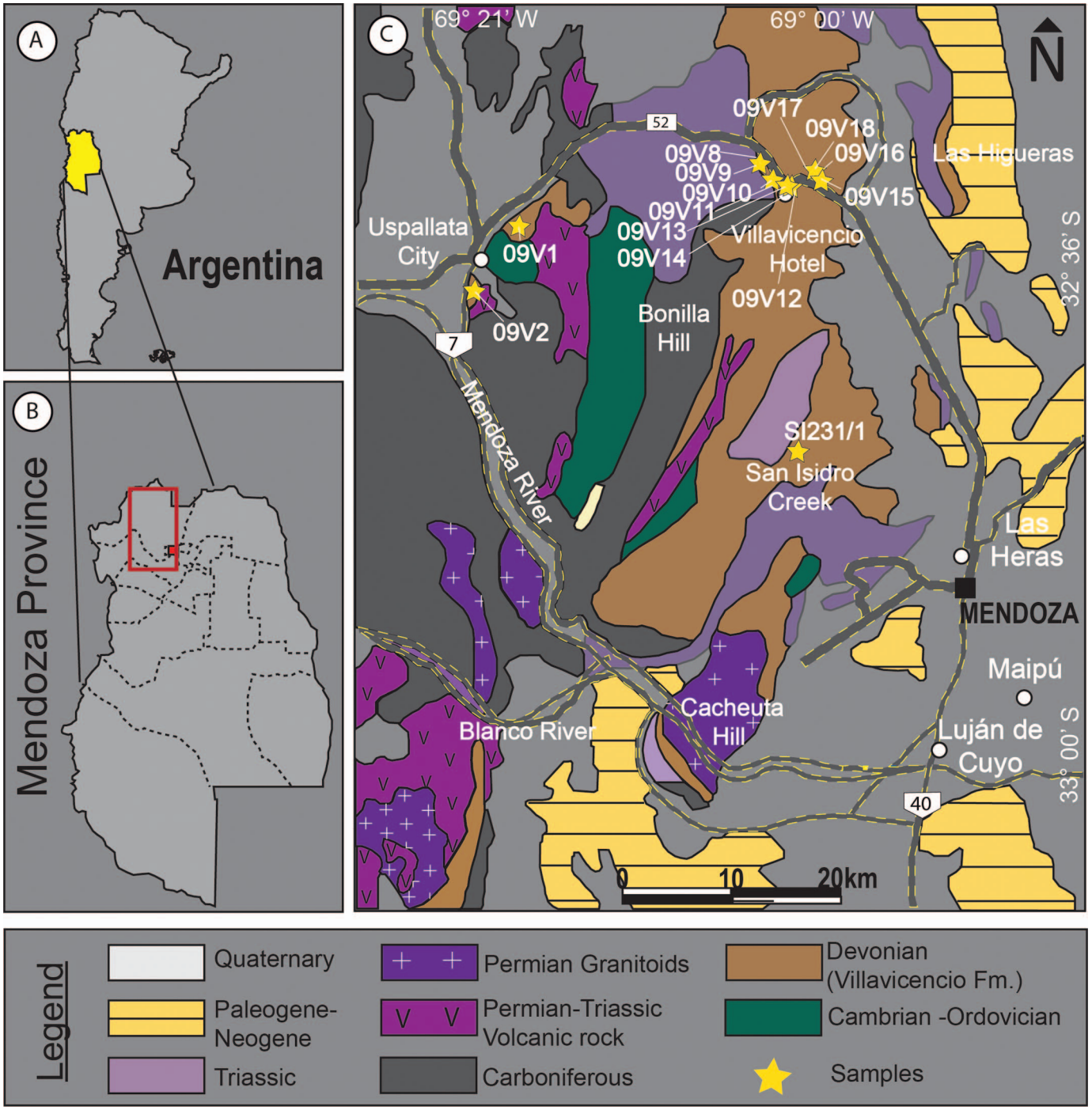

FIG. 2.—Geological sketch map of the study area and the location of collected samples. **A)** Argentina. **B)** Mendoza Province. **C)** Study area and location of samples collected (Modified from Cingolani et al. 2013).

GEOLOGICAL SETTING AND STRATIGRAPHY

The Precordillera structurally developed as a fold and thrust belt related to Neogene Andean deformation associated with subhorizontal subduction, known as the Pampean flat slab (Jordan et al. 1983; Cristallini and Ramos 2000; Ramos et al. 2002, Boedo et al. 2020).

The Precordillera is included within the Cuyania composite terrane (Ramos et al. 1986) with the San Rafael and Las Matras blocks (Fig. 1B). There are two main ideas about the origin of Cuyania. Finney (2007) proposed a para-autochthonous model in which Cuyania would have derived from a southwestern Gondwana position, until the middle Ordovician when it started to migrate to its current position by transform faults generating pull-apart basins where Ordovician sedimentary rocks were deposited. In contrast, the Laurentian microcontinent model proposed by Thomas and Astini (1996) suggests that the Cuyania terrane had rifted from the eastern Laurentian margin during the early Cambrian, drifted

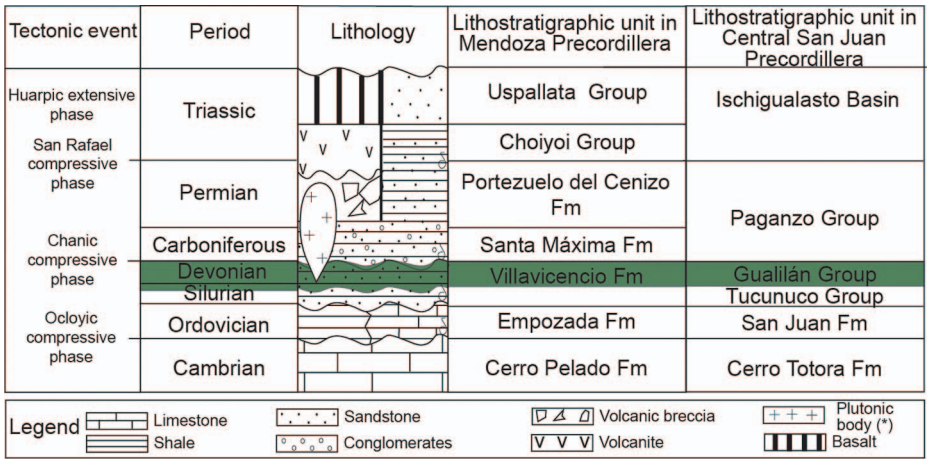

FIG. 3.—Stratigraphic column of the Mendoza Precordillera. Fm, Formation; Gr, Group. Modified from Giambiagi et al. (2010).

along the Iapetus Ocean, and collided with west margin of Gondwana during the Lower–Middle Ordovician Ocloyic orogen. This model has more consensus in several works, such as Benedetto (2004), Naipauer et al. (2010), Thomas et al. (2015), Rapela et al. (2016), and Martin et al. (2020), among others.

According to Keller (1999), the Precordillera extends north from the town of Jagüe (La Rioja), to the city of Mendoza in the south (Fig. 1B). Traditionally, the Precordillera has been divided into three sectors (Western, Central, and Eastern) in the province of San Juan according to its stratigraphic characteristics and tectonic-structural styles (Fig. 1C). Nevertheless, in the north and south of the San Juan province there are two regions with different morpho-structural characteristics and variations on the age of basement, which have received geographical designations: La Rioja Precordillera and Mendoza Precordillera, respectively (Bracaccini 1964; Baldis et al. 1980).

At present, in the eastern sector of the Mendoza Precordillera, the oldest stratigraphic unit includes the Cambrian limestones of the Cerro Pelado Formation (Heredia 1990) and the Ordovician pelites of the Empozada Formation (Harrington 1957) (Fig. 3). Above these units is the late Silurian to early Devonian Villavicencio Formation which is locally intruded by Carboniferous and Permian plutonic bodies. To the north, The Santa Máxima and Jarillal formations, composed of middle Carboniferous to lower Permian marine sediments, continue in strong angular discordance. A middle to late Permian volcanic sequence continues with the lavas and breccias of the Portezuelo del Cenizo Formation, and in discordance the Late Permian to Early Triassic volcanites of the Choiyoi Group.

For the Devonian of the Central Precordillera, the Gualilán Group is formed by the Talacasto (Padula et al. 1967) and Punta Negra (Bracaccini 1949) formations. These thick formations (up to 1000 m each) are made up of fine-grained deltaic sediments. The Punta Negra Formation is characterized by a rhythmic monotonous succession of green sandstones, graywackes, and shales, believed to be equivalent to the Villavicencio Formation (Cuerda and Baldis 1971; Poiré et al. 2005; Arnol and Coturel 2022). In addition, similarities on the fossil content, mainly plant fossils, between the Punta Negra Formation (in the southern sector of San Juan) and the Villavicencio Formation, were pointed out by Edwards et al. (2001, 2009) and Arnol and Coturel (2022) assigning an Early Devonian age.

Devonian deposits in the Mendoza Precordillera extend from the southern boundary of San Juan province to the Mendoza River valley (Fig. 2). These deposits were first recognized by Harrington (1941, 1971) and assigned to the Ordovician. Kury (1993) refers to the unit as Early Devonian based on tectonic observations and plant debris identification. Later, Edwards et al. (2001) identify fossil plants that support the Devonian age established in previous works by other authors (Cuerda et al. 1987; Cuerda 1988; Loske 1992; Kury 1993).

The late Silurian–Early Devonian Villavicencio Formation is widely exposed between the San Juan province to the north and the Mendoza River to the south (Fig. 2) with an approximate thickness of 2000 m. The best outcrops are found east of Uspallata City and surrounding the Villavicencio Hotel. Both the base and top of the unit are limited by faults, therefore, the real thickness of the Villavicencio Formation is unknown (Harrington 1971; Kury 1993). However, the Villavicencio Formation lies in discordance between the Ordovician Empozada Formation and the Permian–Triassic Choiyoi Group (Cuerda et al. 1987). The lithology described for the Villavicencio Formation in the pioneering works (Borrello 1969; Barton and Rodríguez 1989) refers to a rhythmic alternation of massive greenish gray fine-grained sandstones and laminated gray to black shales (conforming heterolithic facies) and gray gravel stones with a low metamorphic grade, which were defined as a flysch-like deposit (Fig. 4A–C). In general, sandstone presents normal gradation, net, or erosional base with current marks and ripples at the base (Fig. 4D, E) indicating E–W and NW–SE paleocurrents (Edwards et al. 2001). The unit yields a diverse paleontological record documented by Cuerda et al. (1987, 1993), Edwards et al. (2001), Rubinstein (1993), and Rubinstein and Steemans (2007). Plant remains were referred to Lycophytes and probably Rhyniophytes. Body fossils include fragments of eurypterids whereas trace fossils include numerous ichnogenera of the *Nereites* Ichnofacies. In addition, palynomorph remains including miospores, sparse chitinozoans, and acritarchs are found in the surroundings of the San Isidro Creek. Pioneering works (Borrello 1969; Barton and Rodríguez 1989 and others) refer to the Villavicencio Formation as a shallow marine platform of sandy nature, while recent works link the deposition to a delta front with a low-energy environment (Poiré and Morel 1996; Cingolani et al. 2013).

SAMPLING AND METHODS

Three sectors were sampled: Uspallata City (samples 09V1 and 09V2), Villavicencio Hotel (09V8, 09V9, 09V10, 09V12, 09V13, 09V14, 09V15, 09V16, 09V17, and 09V18) and San Isidro Creek (SI231/1) (Fig. 2, Table 1). The sampled psammites and pelites were used to carry out analyses of petrography, geochemistry, and Lu-Hf isotopes in detrital zircons, along with morphology and typology determination to estimate the main zircon sources.

Petrography

Petrography analysis is a useful tool for sedimentary rocks to achieve a first approach to provenance studies contributing to the elucidation of possible source areas.

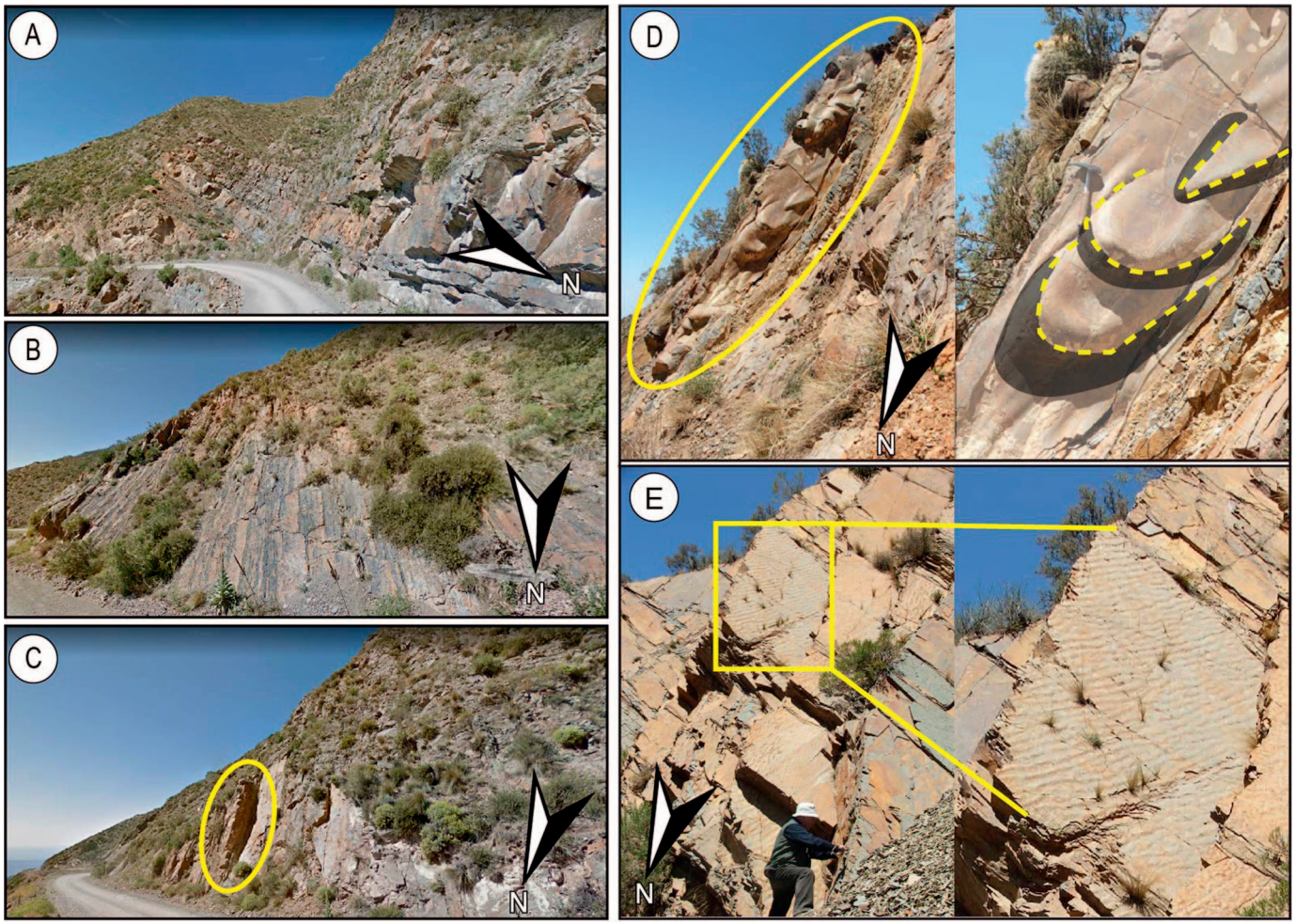

FIG. 4.—**A)** N–S stratification of the Villavicencio Formation (Satellite image, Google). **B)** Characteristic heterolith succession of the Villavicencio Formation (satellite image, Google) **C)** Megaflute identified in the field (Satellite image, Google). **D)** Close up of the megaflutes named before and appreciation of the flow direction towards the North. **E)** Asymmetric ripples with direction from SE towards NW.

Six thin sections of psammites were studied under the microscope (LEICA DM750P), associated with camera (Leica MC170HD), and quantitatively analyzed with a Swift-type point counter (Table 1). Approximately 500 points were counted using the traditional Gazzi-Dickinson method. (Ingersoll et al. 1984).

Classic procedures for petrographic classification of rocks were followed, applying the classification proposed by Garzanti (2016, 2019), and for sedimentary provenance studies ternary diagrams proposed by Dickinson et al. (1983) were used. In addition, the results were compared with similar data known from the Villavicencio Formation (Kury 1993; Cingolani et al. 2013) and the equivalent units Talacasto and Punta Negra formations (Bustos 1995; Arnol et al. 2020, 2022).

Lithogeochemistry

Seven pelitic rock samples (09V9, 09V10, 09V12, 09V13, 09V16, and 09V18) and one psammite sample (09V1) were analyzed. The samples were washed with distilled water, crushed, and pulverized in an agate disk mill at the Museo de La Plata from the Universidad Nacional de La Plata, Argentina. The analyses were carried out under the standard procedures and norms of the Bureau Veritas Commodities Canada laboratory. Major elements were obtained by inductively coupled plasma emission spectroscopy (ICP-ES) on fusion beads. Loss on ignition (LOI) was determined by igniting a sample split and measuring the weight loss. Rare earth elements (REE) and certain trace elements were analyzed by inductively coupled plasma mass spectrometry (ICP–MS). The geochemical data of the supplementary material shows the values of the chemical elements for each sample analyzed.

When normalization is needed, chondrite meteorite values of Sun and McDonough (1989) are used. Likewise, average upper continental crust (UCC) values of McLennan et al. (2006) and the Post-Archean Australian Shales (PAAS) by Taylor and McLennan (1985) were used for comparisons. In addition, the results were compared with the ones obtained for the Gualilán Group in the San Juan Precordillera by Arnol et al. (2020).

Morphologic Analysis of Detrital Zircons

Zircon is a key mineral to understand the geotectonic evolution of a region (Fedo et al. 2003; Anani et al. 2012). Three psammites samples (09V8, 09V14, 09V17) were processed by physical methods (crushing, milling, and sieving) to collect heavy minerals by classical concentration methodologies. The zircon grains were identified and separated under the binocular microscope (Zeiss Stemi 2000-C) by the hand-picking method. Studies of the morphology and typology of the zircon crystals were carried out under the scanning electron microscope (JEOL JSM 6360 LV)

TABLE 1.—*Location, lithology, and the analysis carried out on the collected samples. P, Petrography; GA, Geochemical analysis; MA, Morphology analysis of zircon; CL, Cathodoluminescence; U-Pb, Uranium-lead dating (by Cingolani et al. 2013); Lu-Hf, Lutetium\Hafnium dating.*

Sample	Geographic Coordinate (WGS84)	Area	Lithology	P	GA	MA	CL	U-Pb	Lu-Hf
09V1	S 32° 32′ 55″ W 69° 18′ 47.1″	Uspallata City	Psammite	X	X		X	X	X
09V2	S 32° 37′ 51.5″ W 69° 21′ 05.9″	Uspallata City	Psammite	X			X	X	X
09V8	S 32° 31′ 05.9″ W 69° 02′ 26″	Villavicencio Hotel	Psammite	X		X			
09V9	S 32° 31′ 05.9″ W 69° 02′ 26″	Villavicencio Hotel	Pelite		X				
09V10	S 32° 31′ 18.6″ W 69° 02′ 05″	Villavicencio Hotel	Pelite		X				
09V12	S 32° 31′ 57.3″ W 69° 01′ 23.2″	Villavicencio Hotel	Pelite		X				
09V13	S 32° 31′ 52.2″ W 69° 01′ 28.9″	Villavicencio Hotel	Pelite		X				
09V14	S 32° 31′ 52.2″ W 69° 01′ 28.9″	Villavicencio Hotel	Psammite	X		X			
09V15	S 32° 31′ 12.2″ W 69° 00′ 17.9″	Villavicencio Hotel	Psammite				X	X	X
09V16	S 32° 31′ 12.2″ W 69° 00′ 17.9″	Villavicencio Hotel	Pelite		X				
09V17	S 32° 31′ 14.5″ W 69° 00′ 14.5″	Villavicencio Hotel	Psammite	X		X			
09V18	S 32° 31′ 14.5″ W 69° 00′ 14.5″	Villavicencio Hotel	Pelite		X				
SI231/1	S 32° 52′ 16″ W 69° 01′ 12″	San Isidro Creek	Psammite	X					

at the Museo de La Plata according to the procedures applied by Gärtner et al. (2013) to determine the main morphological populations that are present and a preliminary provenance of the detrital sources (Dickinson and Gehrels 2003). For euhedral zircon grains, the Pupin (1980) classification was used to expand the interpretations. The morphological parameters identified on zircon grains were compared with the data presented by Arnol et al. (2020, 2022) in Devonian sequences of the San Juan Precordillera.

Lu-Hf Detrital-Zircon Analyses

Lu-Hf analysis were conducted on three detrital-zircon samples from the Villavicencio Formation that had been previously analyzed for U-Pb geochronology (Cingolani et al. 2013). Each Lu-Hf analysis consisted of 40 sequential measurements performed in the ICP-MS: 10 with the laser off (measurement of instrumental blank) and 30 with the laser on (laser ablation on GJ-82C and 91500 standards, or the analyte). Each measurement lasted approximately one second. Eight isotopes were measured simultaneously using only Faraday cups: 172, 173, 174, 175, 176, 177, 178, and 180. At the end of each sequence of measurements, the value of the instrumental blank was subtracted from each of the eight isotope signals. Abundance values published by the IUPAC (https://ciaaw.org/pubs/TICE-2009.pdf) were then used to calculate the isotopic ratios between the Yb (172, 173, 174, 176), Lu (175, 176), and Hf (176, 177, 178, 180) signals. Signals 172, 173, and (part of) 174 were used to calculate the fractionation coefficient of Yb (βYb) using exponential law. Signals 180, 178, 177, and (part of) 174 were used to calculate the fractionation coefficient of Hf (βHf) also using an exponential law. As Lu does not have enough isotopes to allow self-correction, the fractionation coefficient of Lu was assumed to be βLu = βHf. The $^{176}Hf/^{177}Hf$ ratio could then be readily obtained after subtracting the two interferences: ^{176}Yb (estimated via βYb) and ^{176}Lu (estimated via βLu) from the 176 total signal. Before and after the analysis, blanks, and zircon standards GJ-82C and 91500 were measured. The analyses of the standards were repeated at regular intervals in order to correct the errors and/or variations of the equipment in the following measurements. Liu et al. (2010) reported a $^{176}Hf/^{177}Hf$ value of 0.282015 ± 0.000025 for the GJ-82C standard, while Woodhead and Hergt (2005) reported an $^{176}Hf/^{177}Hf$ value of 0.282306 ± 0.000006 for the 91500 standard. The parameters εHf and T_{DM} were then calculated using the formulas of Yang et al. (2007). All the U-Pb and Lu-Hf zircon data are provided as supplemental material (U-Pb Data and Lu-Hf Data excel files).

RESULTS AND INTERPRETATIONS

Sandstone Petrography

Psammites of the Uspallata City area (09V1–09V2) are characterized by a range of average grain size of 100 to 150 μm. Grains are angular to subangular, and poorly sorted with abundant matrix (> 35%), resulting in a texturally submature to immature sample. The main components are quartz (monocrystalline and polycrystalline variations), feldspars, and lithics. Monocrystalline quartz is dominant ($\bar{x}$ 19.7%), being also the major component of the matrix. Monocrystalline quartz grains are presented with normal and undulatory extinction. Polycrystalline quartz ($\bar{x}$ 7.5%) is comparatively scarce and occurs in larger crystals of subrounded habit. The potassic feldspars ($\bar{x}$ 4.4%) are recognizable (orthoclase, microclines, and feldspars with perthite) but generally altered to carbonates. Plagioclase ($\bar{x}$ 1.1%), on the other hand, can be found from unaltered to highly altered to carbonates. Lithics are of varied compositions, from low-grade to high-grade metamorphic rocks ($\bar{x}$ 10.1%), intermediate to acid volcanic rocks ($\bar{x}$ 0.6%), and sedimentary psammites and pelites ($\bar{x}$ 0.4%). Muscovite and biotite are also observed ($\bar{x}$ 0.9%), the former being dominant. The presence of chlorite is common. Zircon is the most common accessory mineral. The presence of plant debris was recognized. In addition, the sample 09V2 presents carbonate veinlets, as well as patches of this mineral as cement and a structure that is accompanied by tabular to prismatic components.

According to the diagram proposed by Garzanti (2016), the samples 09V1 and 09V2 are located on the edge between feldspatho-litho-quartzose (fLQ) and litho-quartzose sandstones (Fig. 5). They are distributed in recycled-orogen field for the QFL scheme and transitional or quartzose recycled field in the QmFL triangle (Fig. 5) proposed by Dickinson et al. (1983).

Samples 09V8, 09V14, and 09V17 of the Villavicencio Hotel area have an average grain size of 300 μm. Various textures were identified in the thin-section observations. Samples are poorly to moderate sorted. The matrix content is similar to the samples of the Uspallata City area ($\bar{x}$ 34.6%). The shape of the components is subrounded to subangular. Psammites are dominated by quartz of monocrystalline type ($\bar{x}$ 30.06%) with normal extinction and occasionally undulatory. Some grains show secondary growth (sample 09V8; Fig. 5). Although polycrystalline quartz is not abundant ($\bar{x}$ 4%), it is identified in large grains (Fig. 5). The K-feldspars ($\bar{x}$ 4.33%) present an advanced alteration to carbonates (mainly on the edges), however, it is also possible to recognize distinct species. Moreover, plagioclases ($\bar{x}$ 0.6%) are rarely found to be altered. Low-grade to medium-grade metamorphic lithics are abundant ($\bar{x}$ 23.73%) and

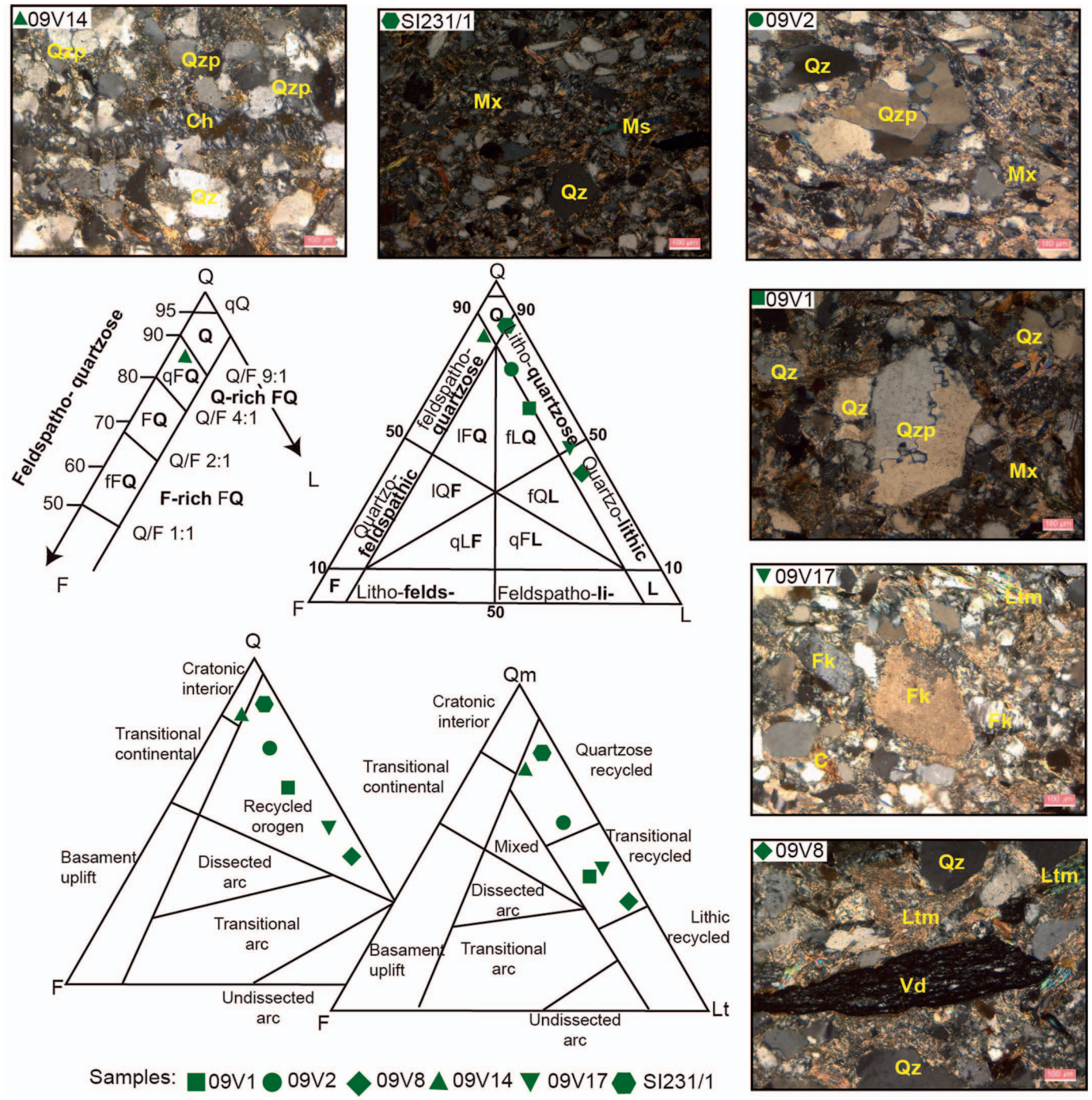

FIG. 5.—Photomicrographs of rock samples from the Villavicencio Formation and their lithological classification according to Garzanti (2016, 2019) and provenance diagram proposed by Dickinson et al. (1983). Qzm, Monocrystalline quartz; Qzp, Polycrystalline quartz; Fk, Potassic feldspar; Ms, Muscovite; Ch, Chlorite; Ltm, Metamorphic lithic; C, Carbonate; Mx, Matrix; Vd, Vegetal debris; F, feldspar; Q, total quartz; Lt, total lithoclasts (including polycrystalline quartz); Qm, monocrystalline quartz; L, lithoclasts.

deformed. It is also possible to recognize sedimentary lithics of pelitic and chert type; sandstone lithics are frequent ($\bar{x}$ 1.6%) (Fig. 5). Nevertheless, sample 09V14 is characterized by the sparse content of lithics (2.6%), which are metamorphic and opaque. Within the phyllosilicates, muscovites, biotites, and dispersed crystals of chlorites can be distinguished ($\bar{x}$ 0.53%). Some muscovites are altered to chlorite and to clay minerals. Sample 09V17 contains sericite which has an ochre coloration. The presence of plant debris is observed (Fig. 5). The cement in samples 09V14 and 09V17 is rich in clay minerals with occasional carbonate. In addition, opaque minerals were recognized in these samples.

The samples of the Villavicencio Hotel area are classified according to Garzanti (2016, 2019) as: quartzo-lithic (09V8), feldspatho-quartzose/qFQ: quartz-rich (09V14), and litho-quartzose (09V17) (Fig. 5). They are distributed between the transitional recycled orogen and quartzose recycled

orogen fields for the QmFLt scheme and recycled orogen in the QFL triangle proposed by Dickinson et al. (1983) (Fig. 5).

Finally, the sample of the San Isidro Creek (SI231/1) has an average grain size of 100 μm. The high concentration of matrix (> 35%) allows the rock to be defined as a texturally immature rock. A preferential grain orientation is observed. Compositionally, 11.8% of the framework grains correspond to monocrystalline quartz and 1% to polycrystalline quartz, both with undulatory extinction; oxides, 0.6% plagioclases, 0.6% potassium feldspars, and sedimentary lithics (1.4%) and carbonate lithics (6%) were recognized (Fig. 5). Among the components of the matrix, the presence of muscovite and biotite is highlighted.

The sample is in the quartzose field of Garzanti (2016) (Fig. 5). It is distributed in the quartzose recycled field for the QmFL scheme and recycled orogen in the QFL triangle proposed by Dickinson et al. (1983) (Fig. 5).

Geochemistry

The whole-rock geochemical composition of a sedimentary rock provides valuable information on the detrital nature, provenance, and evidence to understand the tectonic environment of the depositional basin, considering in turn the possible influences of factors such as weathering, diagenesis, and metamorphism (Cullers 1995). Geochemical analyses applied to fine clastic sedimentary rocks for provenance purposes allow for identification of constituents that might be important for tectonic interpretations which cannot be achieved by petrography due to grain size (Hessler and Fildani 2019). For the present work, pelites from the Villavicencio Hotel (09V9, 09V10, 09V12, 09V13, 09V16, 09V18) area are mainly analyzed, except for sample 09V1 (Uspallata City area), which corresponds to a medium grain-sized psammite; such grain-size difference explains its differential behavior in all diagrams presented (Fig. 6).

Weathering.—The Chemical Index of Alteration (CIA), as established by Nesbitt and Young (1982), is currently the most widely used index for mobile major elements, because it is the one that supplies the greatest inferences as to the weathering undergone by a rock (Bahlburg and Dobrzinski 2011). The CIA values obtained ranged from 67.2 to 75.5. The proximity of these values to those of the PAAS (Nance and Taylor 1976) indicate null to incipient weathering action. Some samples display K-metasomatism (plotting towards the illitic field in the A-CN-K diagram in Fig. 6A) and deviate from a normal weathering trend expected for rocks derived from sources with an average UCC composition due to K_2O enrichment (UCC value of 3.4% according to McLennan et al. 2006). See geochemical data in supplemental materials.

The Th/U ratio is another useful tool for estimating weathering and recycling from source rocks (McLennan et al. 1993). A Th/U ratio of 3.5 to 4, similar to the UCC of 3.8 (McLennan et al. 1993), indicates low weathering and/or recycling. Under conditions of oxidation this ratio increases due to the transformation of (U^{+4}) to more mobile and soluble forms (U^{+6}). Low Th/U ratios are typical of rocks derived from mafic sources, although they may be due to an enrichment in the latter element (McLennan 1989) linked to secondary sedimentary processes related to environmental conditions. Figure 6B shows Th/U ratios rather typical of rocks derived from sources with average UCC composition, with low weathering and/or recycling, in agreement with CIA values; nonetheless enrichment in the U content with values of up to 10.4 ppm are indicative of U gain probably linked to reducing (anoxic) environmental conditions that not only prevented U from oxidiz but favored its concentration (Dypvik and Harris 2001; Mouro et al. 2017; Rakociński et al. 2016).

Source Compositions.—The REEs represent reliable provenance indicators, as they would reflect the average REE composition of the source material (McLennan 1989). The chondrite normalized REE patterns are parallel to the PAAS, despite certain enrichment in HREEs, confirming derivation from sources with an average composition similar to UCC; Eu [EuN/(0.67SmN) + (0.3TbN)] and Ce [CeN/(0.67LaN + 0.33NdN)] anomalies show similar and parallel patterns confirming the resemblance and origin of crustal-like sources (Fig. 6C).

The Cr/V and Y/Ni ratios are useful to evaluate the provenance of ophiolitic sources (McLennan et al. 1993) As shown in Figure 6D, these ratios of the Villavicencio Formation indicate that an ophiolitic source can be ruled out, reinforcing the idea that the elevated Uranium content is due to secondary enrichment.

The Th/Sc ratio is a provenance proxy that distinguishes felsic from mafic sources. The Zr/Sc ratio, in turn, allows evaluation of the recycling, since the Zr concentration is directly related to the zircon content (McLennan et al. 1993). Figure 6E illustrates the Th/Sc ratios cluster around average UCC composition; Zr/Sc ratios are not indicative of recycling, except for sample 09V1, which shows some reworking. The same information can be deduced using the La/Th ratios vs Hf concentration (Fig. 6F).

Morphologic Analysis of Detrital Zircons

The analysis of zircon morphology from SEM images, combined with other studies (CL images, and chemical and isotopic composition of U-Pb and Hf) allow estimation of the source of the crystals (Pupin 1980; Heaman et al. 1990; Gärtner et al. 2013). The study of zircon population typology is an important insight, since this mineral has high resistance in sedimentary environments, and its morphology is controlled by the physical and chemical conditions under which it crystallized (Anani et al. 2012).

Zircon Morphology.—Samples 09V8, 09V14, and 09V17 come from the Villavicencio Hotel area. Based on the classification of Gärtner et al. (2013), most of the crystals present a stubby and subordinately stalky habit. Very few of them have a prismatic habit, and none with a needle-like habit are present (Fig. 7A). Likewise, most of them show collision marks corresponding to the lowest degree of impacts (grade I), while a small percentage (~ 10%) are affected by more severe collisions (grades III and IV) (Fig. 7B). An important number of crystals (> 50%) are fractured; most of them show sharp fractures (~ 78%) with defined limits, and others show fractures with rounded edges (Fig. 7C). The degree of roundness is variable, where most of the population is poorly rounded (class 4), followed by fairly rounded to rounded subpopulations (classes 5 and 6, respectively). To a lesser extent, very well rounded (class 8), almost completely rounded (class 9), to completely rounded (class 10) zircon grains appear (Fig. 7D). The crystal typologies recognized according to the parameters of Pupin (1980) are P4 with a predominant population and S19-S24-S25-P5 are present in a subordinate way (Fig. 7E).

Cathodoluminescence.—From cathodoluminescence images, it is possible to visualize the internal structure of the crystals, which is a consequence of their geological history (Uriz et al. 2022, and references therein). A magmatic origin can be recognized when internal oscillatory zoning is partially or completely distributed within the grains. A mostly high-grade metamorphic origin may become recognizable due to completely homogeneous internal zircon structures associated with slow diffusion from slow crystal growth (Watson and Liang 1995; Watson 1996). Recrystallization events that can be related to both plutonic and metamorphic origin are denoted by the heterogeneous zoning present in the crystals (Uriz et al. 2022).

Most of the zircon grains analyzed for the three samples exhibit internal structures with normal and concentric zonation that could be associated with plutonic-type magmatic sources; few grains presented cores inherited from previous crystallizations (1284–1135 Ma) with recrystallized rims of 1033–989 Ma, which could be associated with a metamorphic origin (Fig. 8). Few dissolution features are present. Nevertheless, it is worth

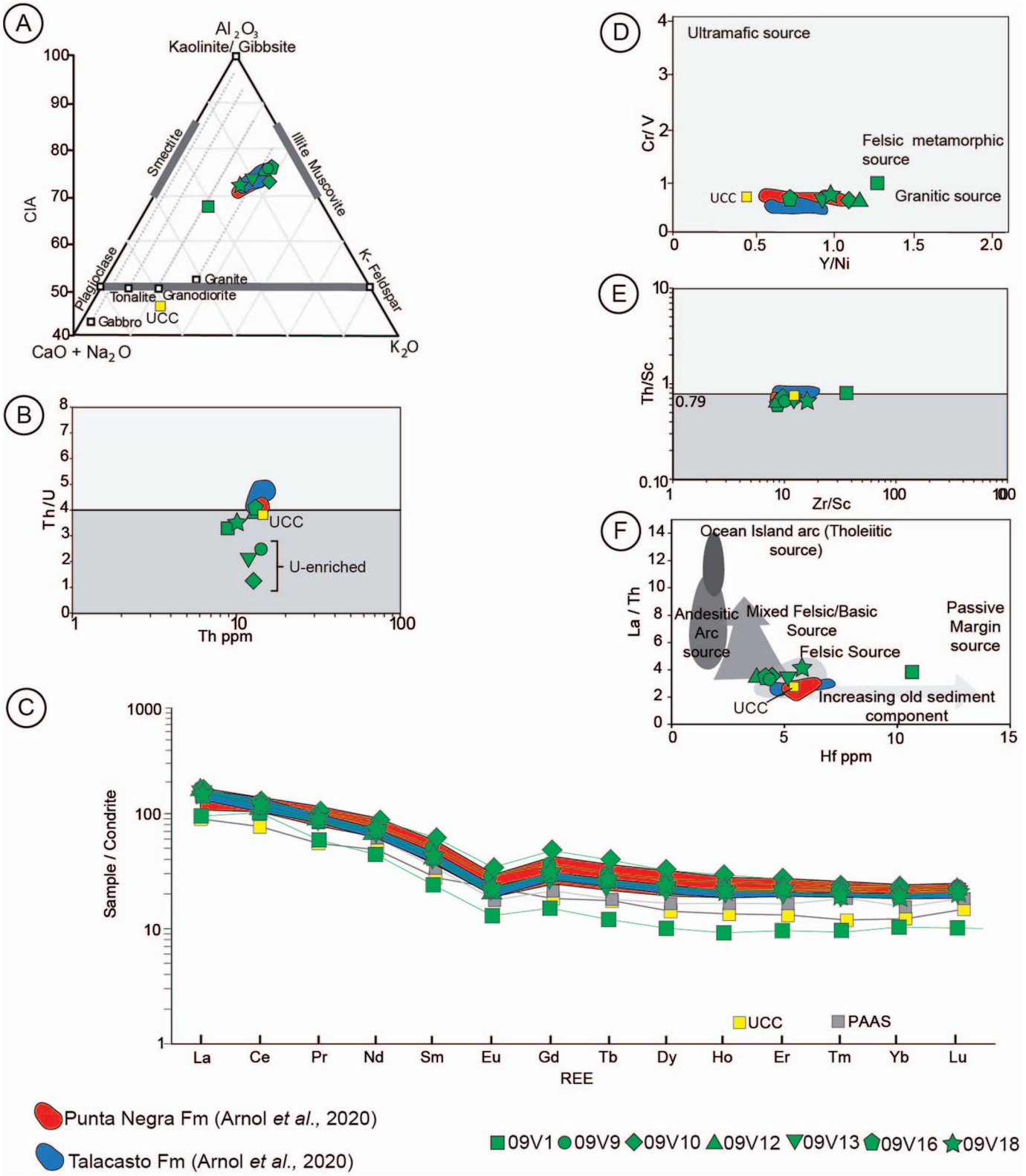

FIG. 6.—**A)** Aluminium–Calcium + Sodium–Potassium (A-CN-K) diagram based on molecular proportions and CIA (Nesbitt and Young 1984, 1989) scale on the left; UCC and idealized mineral compositions are according to Taylor and McLennan (1985). **B)** Th/U ratio vs. Th (ppm) modified from McLennan et al. (1993) **C)** Concentrations of REE compared to the Post Archean Australian Shales (PAAS) by Taylor and McLennan (1985) and to the average content of the Upper Continental Crust (UCC) from McLennan et al. (2006). **D)** Cr/V vs Y/Ni relationship by Hiscott (1984) and McLennan et al. (1993) **E)** Th/Sc vs Zr/Sc relationship modified from McLennan et al. (1993). **F)** La/Th vs. Hf diagram (Floyd and Leveridge 1987).

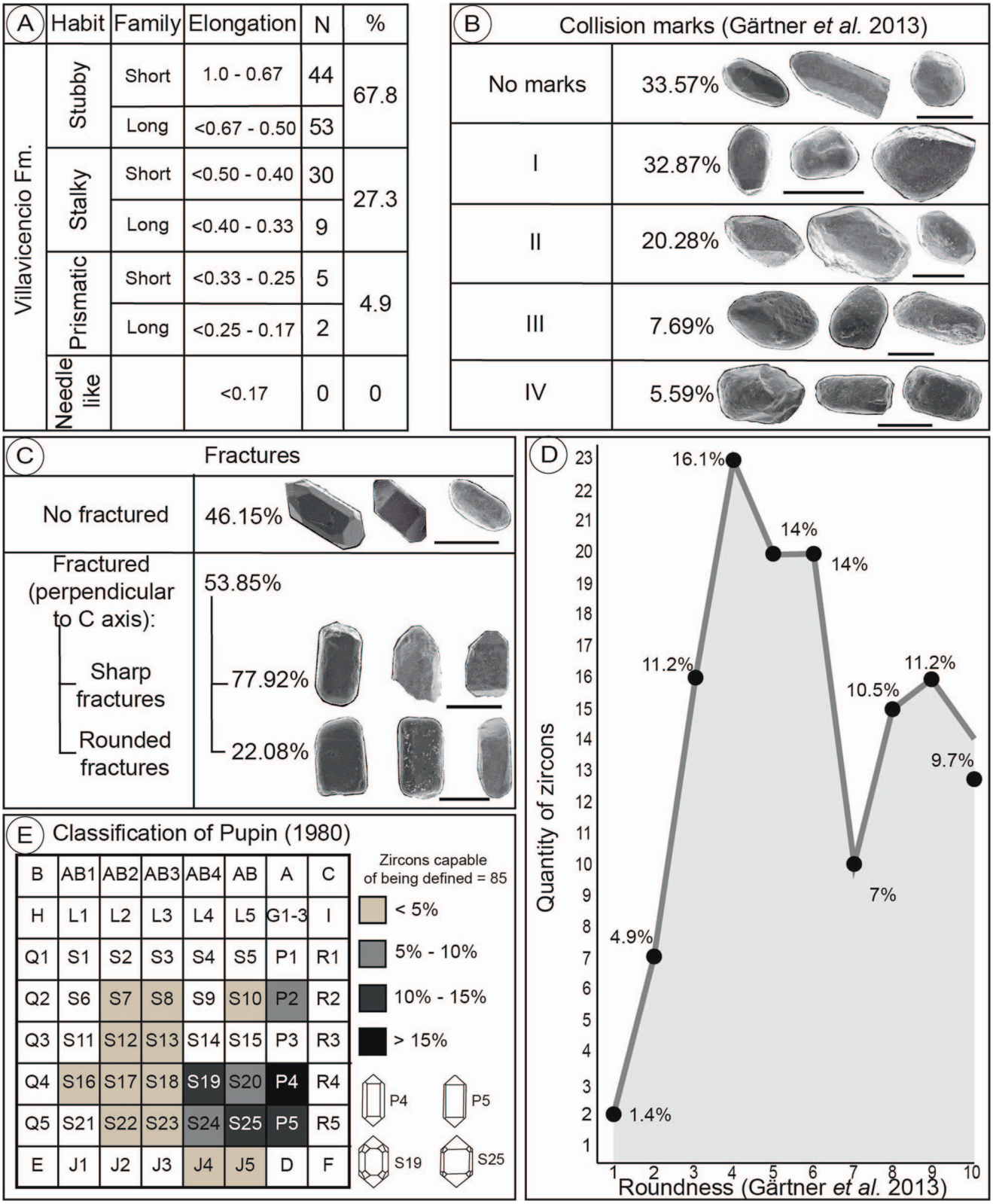

FIG. 7.—Morphological classification of zircons (based on Gärtner et al. 2013). **A)** Habit. **B)** Collision marks. **C)** Fractures. **D)** Roundness. **E)** Typological classification according to Pupin (1980).

noting the degree of fracturing of the crystals, where more than 90% are fractured preferentially perpendicular to the C axis. Although a large part of the crystals shows rounded edges, these crystals are fragments of zircon grains.

In summary, dominance of short and subordinately stalky elongations is associated with a plutonic origin, whereas the very few multifaceted crystals are related to a metamorphic origin. Main zircon morphotypes point to calc-alkaline magmas (Pupin 1980) from which hybrid granites with both crustal and mantle origin would have crystallized (Daneshvar et al. 2018). This is also supported by the Th/U ratios and the cathodoluminescence records which show a majority of crystals with concentric zonation and to a lesser content metamorphic origin (Cingolani et al. 2013; Arnol et al. 2022).

Lu-Hf Isotope Data

In previous works, Cingolani et al. (2013) reported the U-Pb ages of detrital zircon grains from three samples (09V1 and 09V2 from the Uspallata region and 09V15 from the Villavicencio Hotel area). In this contribution, detrital zircon populations with Paleoproterozoic, Mesoproterozoic, Neoproterozoic, and Paleozoic ages are analyzed using the Lu-Hf methodology to establish the characteristics of the magma from which they derived. Detailed data can be consulted in the Lu-Hf data in the supplemental materials, although the results obtained are summarized below and illustrated in Figure 9.

Paleoproterozoic U-Pb ages are between 2289 and 1673 Ma. The T_{DM} parameter indicates a range from 3600 Ma to 2400 Ma, indicating a derivation from Archean and Paleoproterozoic crust. The εHf record values from 0 to −13, indicating a high residence time in the crust, with marked differentiation.

Zircon grains with Mesoproterozoic U-Pb ages are divided into three groups for this study; four zircon grains with Calymmian U-Pb ages (1600–1400 Ma) show that the εHf parameter ranges between 10 and 2 with TDM model ages from 2000 Ma to 1600 Ma indicating less crustal residence time, preserving the juvenile characteristics of the original magma. On the other hand, 13 zircon grains represent the Ectasian (1400–1200 Ma), with a range of εHf values between 12 and 3 and the model ages ranging from 1800 Ma to 1400 Ma. A single crystal (1243 Ma) showed characteristics dissimilar from the rest with an εHf value −1 and T_{DM} 2000 Ma. Stennian ages (1200–1000 Ma) represent the largest group of zircon grains analyzed, with a total of 33 crystals. The pattern values in this group proved to be homogeneous with T_{DM} between 1900 Ma to 1100 Ma, while εHf values vary between 12 and 0. A single zircon exhibits characteristics that are inconsistent with the rest of the group as its εHf value −5 and T_{DM} 2010 Ma. In all cases a few crystals are derived from poorly evolved magmas with juvenile characteristics.

Neoproterozoic ages comprise seven zircon grains, of which five of them correspond to the Tonian (1000–720 Ma) and two to Ediacaran ages (635–538 Ma). In the first group, four crystals present homogeneous behaviors with T_{DM} between 1628 Ma and 1500 Ma and εHf values between 3 and 2. The remaining Tonian zircon is close to the model age of this crystal on the boundary with the Cryogenian (1100 Ma) and the value of εHf is 8. The crystals of Ediacaran ages show large parameter dispersion. The oldest crystal at 581 Ma, yielded a T_{DM} of 2180, and the εHf(t) is −11. The youngest grain (547 Ma) generated T_{DM} values of 900 Ma and εHf(t) 8.

Zircon grains of Paleozoic ages are between the Early Cambrian and the Silurian (538–419 Ma) and have seven analyzed crystals. The zircon grains of Early Cambrian age present a homogeneous behavior in the values of the considered parameters; the T_{DM} varies between 2100 Ma and 1400 Ma, while the εHf(t) fluctuates between −1 and −13, indicating an important crustal contamination. The Ordovician zircon grains differ from the Cambrian zircon grains by presenting younger model ages between 1600 Ma to 1000 Ma, and εHf(t) between 5 and −4, evidencing a greater heterogeneity in the sediment sources. Finally, the only zircon of Silurian age (429 Ma) presents a T_{DM} value of 1200 Ma and an εHf(t) of 2, indicating a juvenile component.

COMPARISON WITH THE GUALILÁN GROUP AND DISCUSSION

Provenance interpretations can be made with the information obtained in this work and its comparison with former work in the Precordillera geological province (Kury 1993; Bustos 1995; Cingolani et al. 2013; Arnol et al. 2020, 2022).

Petrography

In agreement with the observations of Cingolani et al. (2013), the psammitic deposits of the Villavicencio Formation have a higher matrix content than those of the Punta Negra Formation (Central San Juan Precordillera) (Bustos 1995; Arnol et al. 2020, 2022). The samples with the finest grain sizes are from the western and southern part of the study area from the San Isidro Creek and Uspallata City localities (Fig. 2). The main component is quartz, which is present in its two varieties, monocrystalline and polycrystalline, the former being dominant. The appearance of plant debris to the north (09V1, 09V2, 09V8, 09V17) accompanied by a coarser grain size to the east and the general high content of matrix may imply continentalization towards the northeast.

The provenance diagrams of Dickinson et al. (1983) are useful to compare data from our samples with that of the Villavicencio Formation from previous work (Kury 1993; Cingolani et al. 2013) and with the Gualilán Group in the Central San Juan Precordillera (Bustos 1995; Arnol et al. 2020; 2022). Results presented here are in accordance with the dominantly recycled orogen provenance, particularly linked to a transitional recycled orogeny as determined by Kury (1993), rather than to a mixed area as proposed by Cingolani et al. (2013). Regarding the Gualilán Group in San Juan province (data from Arnol et al. 2020, 2022), the best matches are with the uppermost unit of the group, the Punta Negra Formation (Fig. 10).

Following Garzanti (2016), the Villavicencio Formation is linked to a recycled clastic provenance, characterized by a significant metamorphic lithic content. Despite the impossibility of distinguishing between autochthonous or allochthonous continental crust, a tectonic setting linked to an already collided source area exhumed by the Devonian can be inferred for the depositional timing of the Villavicencio Formation. The possible action of turbiditic deposits (following Garzanti 2019), or rather hyperpycnal flows (following Zavala et al. 2021) in a deltaic environment, is reinforced by the presence of aligned plant debris observed in the thin sections and the plant descriptions made by Edwards et al. (2001). Sedimentary structures show a dominance of unidirectional paleocurrents mainly from east to west, although the presence of bidirectional paleocurrents E–W and NW–SE is subordinate (Edwards et al. 2001; Cingolani et al. 2013).

Geochemistry

Geochemical analyses indicate that the Villavicencio Formation is moderately weathered and is derived from sources with an average unrecycled UCC composition, lacking evidence of important depleted source rock(s). Data are similar to those obtained for the Gualilán Group (Fig. 6) by Arnol et al. (2020), particularly to the Lower–Middle Devonian Punta Negra Formation, which would represent the proximal facies.

As far as the concentration of uranium is concerned, it can reflect reducing environmental conditions, i.e., dysoxic and even anoxic environmental conditions (Dypvik and Harris 2001; Rakociński et al. 2016; Mouro et al. 2017). A deltaic environment (Poiré and Morel 1996) with low-energy regime (Cingolani et al. 2013) is interpreted for the Villavicencio Formation, in which oxygen scarcity allowed concentration

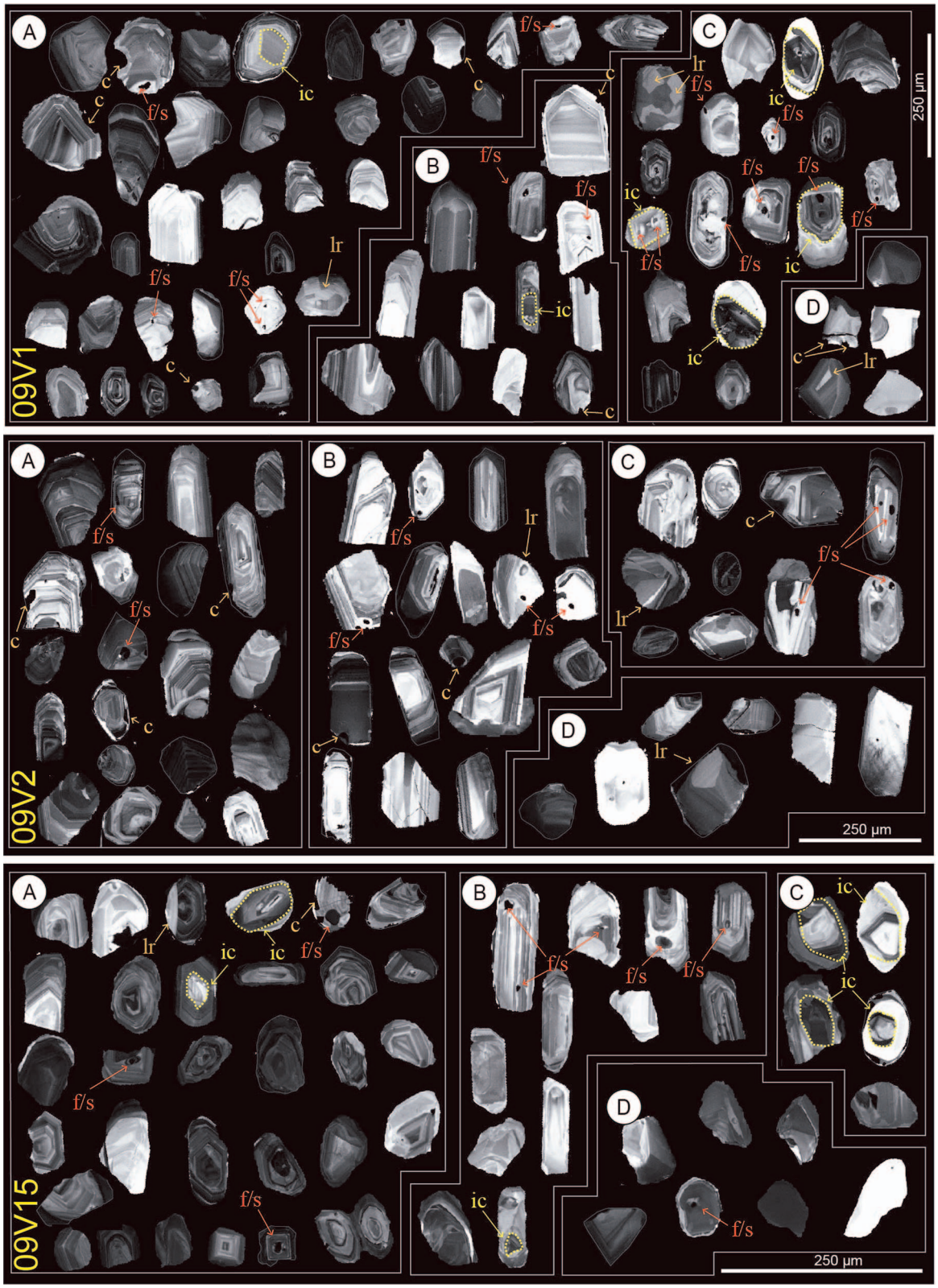

FIG. 8.—Selection of the cathodoluminescence images of detrital zircon grains from the analyzed samples of Villavicencio Fm. ic, inherited core; lr, local recrystallization; f/s, fluid or solid inclusions; c, corrosion or dissolution. **A)** Internal oscillatory zoning, **B)** simple broad zoning, **C)** convolute zoning. **D)** Internally homogeneous zircons.

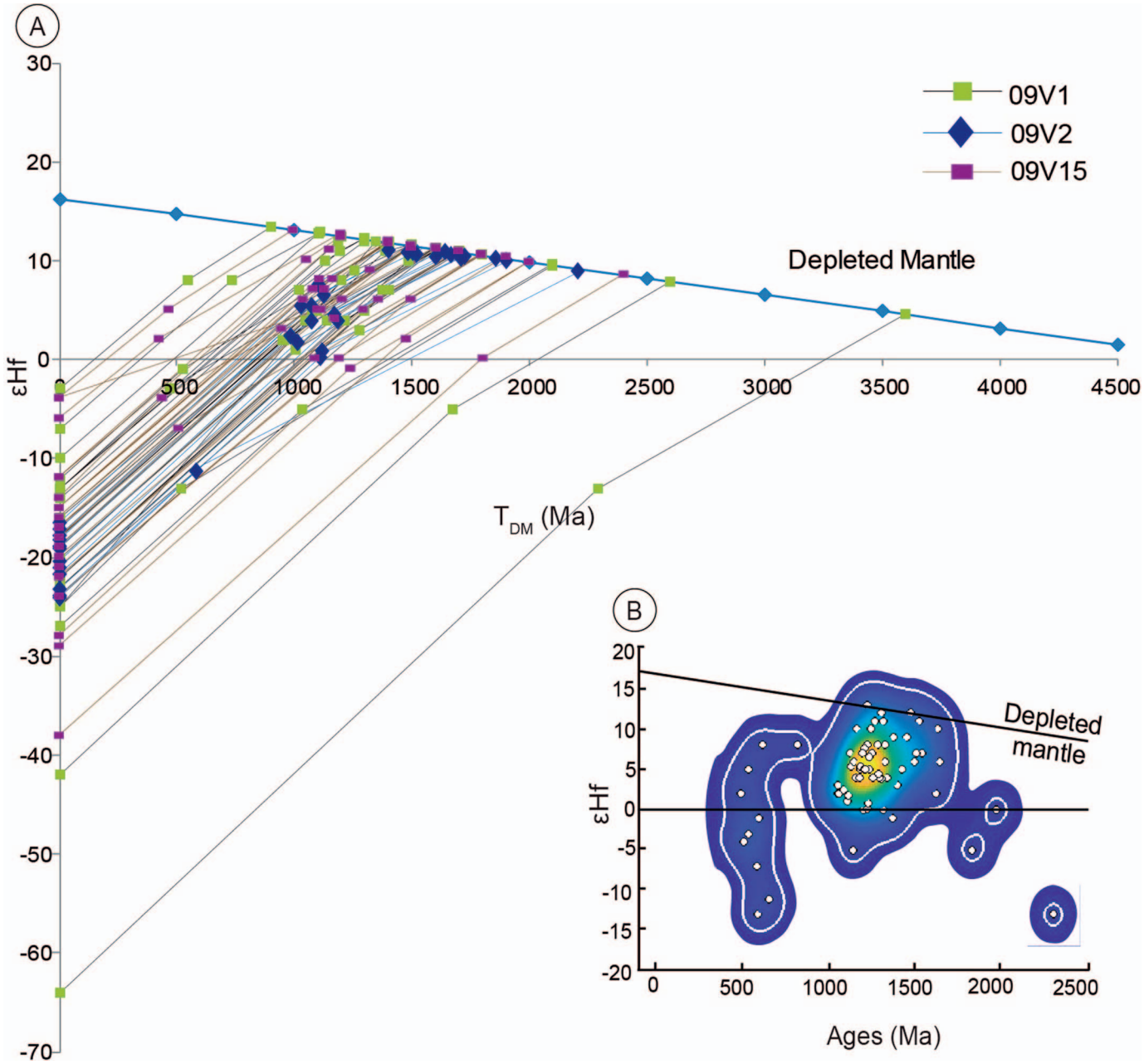

FIG. 9.—**A)** εHf (t) evolution diagram showing results for the Villavicencio Formation. **B)** Kernel diagram showing the distribution and concentration of the U-Pb age (LA-ICP-MS) of zircons with their respective εHf.

of uranium within a low-energy distal delta front–prodelta–offshore environment. The presence of continental plant debris and sedimentary structures would indicate the action of episodic hyperpycnal flows.

Morphologic Analysis of Detrital Zircons

Zircon crystal morphological patterns are like those observed in the Gualilán Group in San Juan Province (Arnol et al. 2020, 2022). However, the higher degrees of rounding (classes 8, 9, and 10) expressed in the minor peak of the Villavicencio Formation (Fig. 7D) have a higher involvement than the Gualilán Group. This rounding may be due to resorption of metamorphic fluids (Malusà et al. 2013) or fluvial transport (Gärtner et al. 2013). Although the first process has greater support due to laboratory evidence, resorption of metamorphic fluids is not considered, inasmuch as the authors assign this process to regional metamorphism. If so, the Villavicencio and Punta Negra samples should have the same characteristics. In addition, the fact that the total of zircon grains analyzed show variability in the degree of roundness (Fig. 7D), collision marks (Fig. 7B) in most, and cathodoluminescence that shows no evidence of the prominence of metamorphism (Fig. 8) confirmed by Th/U ratios, support fluvial transport.

U-Pb Ages and Statistical Correlation

The first attempt to identify the probable source rock(s) of the Villavicencio Formation based on zircon morphology was carried out by

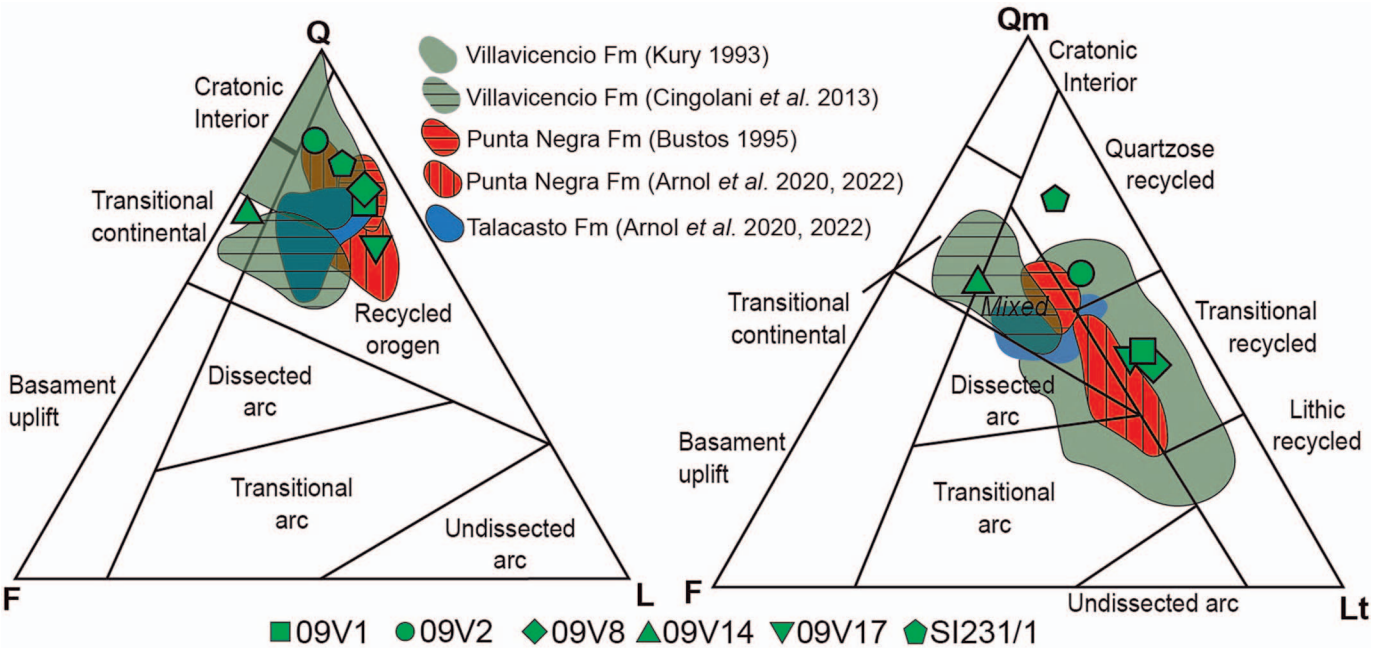

FIG. 10.—Provenance ternary diagrams after Dickinson et al. (1983) showing compositional distribution of the samples from the Villavicencio Formation in the present work, from Kury (1993) and Cingolani et al. (2013), and data for the Gualilán Group (Talacasto and Punta Negra formations) from Bustos (1995) and Arnol et al. (2020, 2022). F, feldspar; Q, total quartz; Lt, total lithoclasts (including polycrystalline quartz); Qm, monocrystalline quartz; L, lithoclasts.

Loske (1992, 1994). This author suggested a provenance of granitoid source rocks, present in several areas near the Precordillera, such as the Sierra de Pie de Palo, with U-Pb TIMS Grenville crystallization ages of approximately 1100 Ma (Stennian). The contributions of Cingolani et al. (2013) with U-Pb ages (Fig. 11) confirm the dominance of Mesoproterozoic populations (between 72% and 83% of the zircon-grains U-Pb age distribution) of which about half of them correspond to Stennian ages (1200–1000 Ma), subordinate (18–24%) Ectasian (1400–1200 Ma), and scarce participation (< 4%) of the Calymmian (1600–1400 Ma). Therefore, the main contributions are from the Grenvillian Cycle (ca 1300–1000 Ma). The Pampean–Brazilian Cycle (ca 800–521 Ma) is represented by 8–14% of the zircon grains being dominantly Neoproterozoic over Lower Cambrian. Finally, the Famatinian (ca 520–360 Ma) and Transamazonian (ca 2200–1800 Ma) cycles are scarce, constituting less than 9% and 5% of the populations, respectively. The oldest data correspond to the Paleoarchean at 3523 Ma, while the youngest is from the middle Silurian at 429 Ma (Wenlockian). In comparison with the data provided by Arnol et al. (2020, 2022) for the Gualilán Group, the Talacasto Formation shows variable percentages and dominances between the Grenvillian (22.5–37.6%), Pampean–Brazilian (20.3–36.6%), and Famatinian (17.5–45.6%) cycles, whereas the Punta Negra Formation shows a clear predominance of Mesoproterozoic ages associated with the Grenvillian Cycle. However, towards the northernmost sector, the samples manifest lesser Mesoproterozoic detrital zircon grains (52.1–58.4%) with no correlation compared to samples from the middle and southern sector of the same unit (Arnol et al. 2020, 20222). The Villavicencio Formation has a strong correlation with the samples of the Punta Negra Formation, specifically with those from the central part of the basin, suggesting the same debris supply (Arnol et al. 2022). The U-Pb ages of Villavicencio Formation present values similar to those of Arnol et al. (2022) for the Punta Negra Formation. Between 72 and 94% are contained within Mesoproterozoic populations, followed by Pampean–Brazilian cycle with values less than 23%, the Famatinian cycle (< 5%), and a single sample in this sector with scarce Transamazonian (3.4%). Following the proposal of Arnol and Coturel (2022) that the Villavicencio Formation and Punta Negra Formation are equivalent units based on paleoflora, the distribution of U-Pb ages support this idea. In addition, as most of the zircon crystals had a Mesoproterozoic age, they evidence the exposure of the older and deeper rocks (Arnol et al. 2022). Figure 11 reflects all the data mentioned above for the Villavicencio Formation and the comparison with the data from northern samples of Arnol et al. (2020, 2022).

From the dominance of Grenvillian ages in U-Pb dating, the western Pampean Ranges (such as the Sierra de Pie de Palo, Umango, Maz, and Espinal) are established as the main sediment source area (Galindo et al. 2004; Rapela et al. 2010, 2016; Varela et al. 2011; Cingolani et al. 2013; Ramacciotti et al. 2015; Arnol et al. 2020, 2022).

Lu-Hf Distribution

Arnol et al. (2022) showed a predominance of Mesoproterozoic zircon grains for the Punta Negra Formation with positive εHf values (juvenile-mantle origin) from crusts originating in this same period, indicating that they did not experience significant contamination (Fig. 12B). On the other hand, the Talacasto Formation presents εHf values close to zero and large variability between positive and negative values. These ambiguous provenance signatures mean that it is not possible to define a particular origin (Fig. 12C). Nevertheless, considering the period between 1500 and 1000 Ma, the εHf values are generally positive, indicating Mesoproterozoic juvenile sources, while for ages around 500 Ma (Pampean–Brazilian Cycle), the sources for the three units are more heterogeneous. Although the proportion of ages varies among the three successions, the sources are the same (Mesoproterozoic, Pampean–Brazilian, and Famatinian mainly). This variation could be due to distinct positions in the basin or to the deposition in sub-basins separated by local highs ("Arenas High," see Arnol and Coturel 2022 and references therein); this means that the changes would be more related to paleorelief controls, in addition to a segmentation of the Mesoproterozoic orogens in the northern depocenter of the basin rather than to tectonic changes in the large-scale paleogeography (Fig. 13).

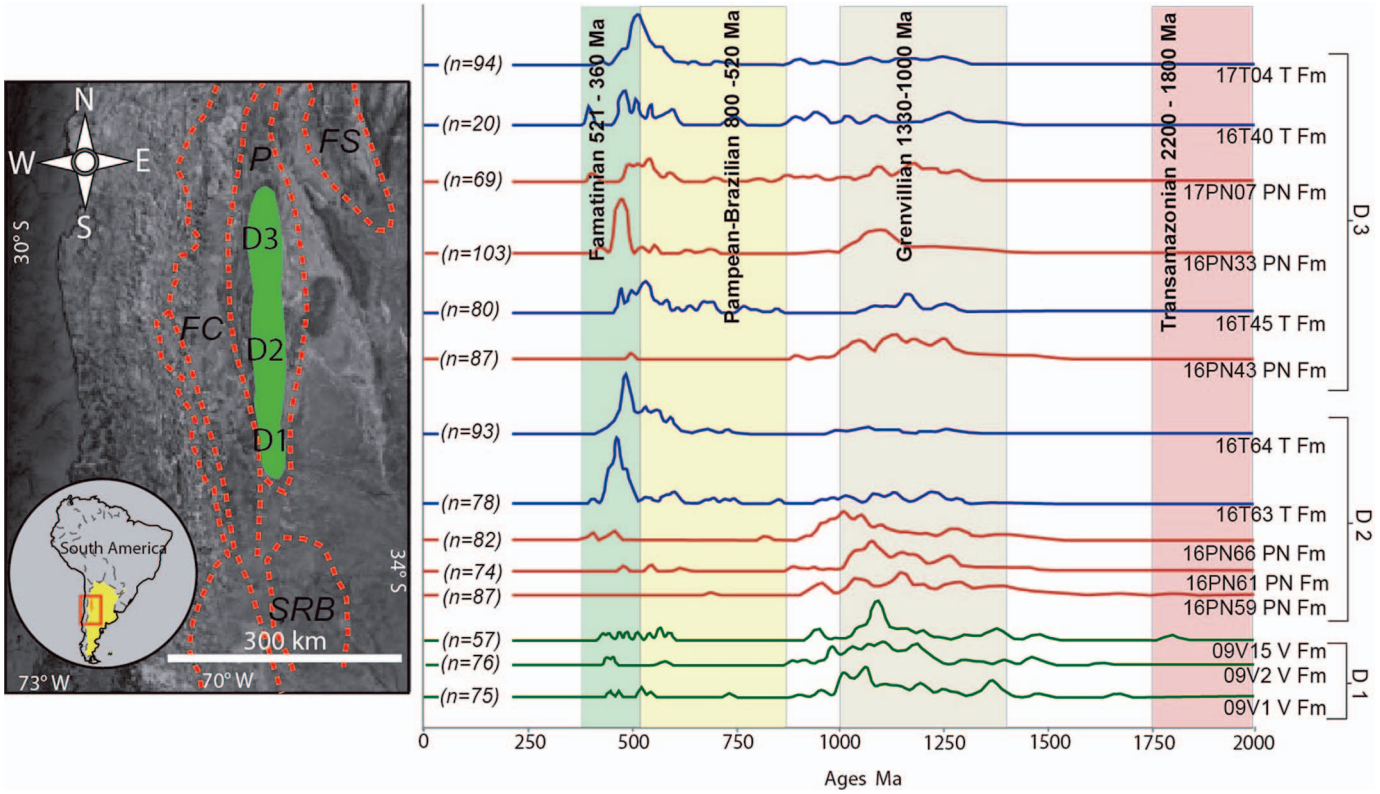

FIG. 11.—U-Pb age distributions along the Devonian basin of the Mendoza and Central San Juan Precordillera. D1 data from Cingolani et al. (2013), D2 data from Arnol et al. (2020), D3 data from Arnol et al. (2022). FS, Famatina System; P, Precordillera; FC, Frontal Cordillera; SRB, San Rafael Block; PN, Punta Negra Formation; T, Talacasto Formation; V, Villavicencio Formation.

The hypothesis that the Villavicencio Formation and the Punta Negra Formation are equivalent units is supported by a variety of aspects: 1) The petrographic similarity highlighting the abundance and types of metamorphic lithics and the presence of plant debris, 2) the geochemical similarities such as CIA values and the composition of the sedimentary sources that reflect non-recycled UCC, with no reworking and no depressed sources, 3) the resemblance of zircon morphology, 4) the U-Pb ages recorded, 5) and the εHf patterns in specific time lapses. All of this suggest that the Villavicencio Formation and the Punta Negra Formation have the same sediment source and could have been part of the same basin (Fig. 13). The Villavicencio Formation was deposited during the late Silurian–Early Devonian within a peripheral-foreland-basin geotectonic setting that developed after the collision of the allochthonous Cuyania Terrane along the southwestern margin of Gondwana (Dalla Salda et al. 1992; Dalziel et al. 1994; Astini et al. 1995; Dalziel 1997). The main contribution of detritus corresponds to igneous–metamorphic basement rocks with Grenville ages and positive εHf values interpreted as derived from the Western Pampean Ranges (Fig. 13). This is confirmed by Lu-Hf analysis from the Maz and Pie de Palo complexes (see Martin et al. 2020). This implies that by the Devonian, the source area was already exhumed,

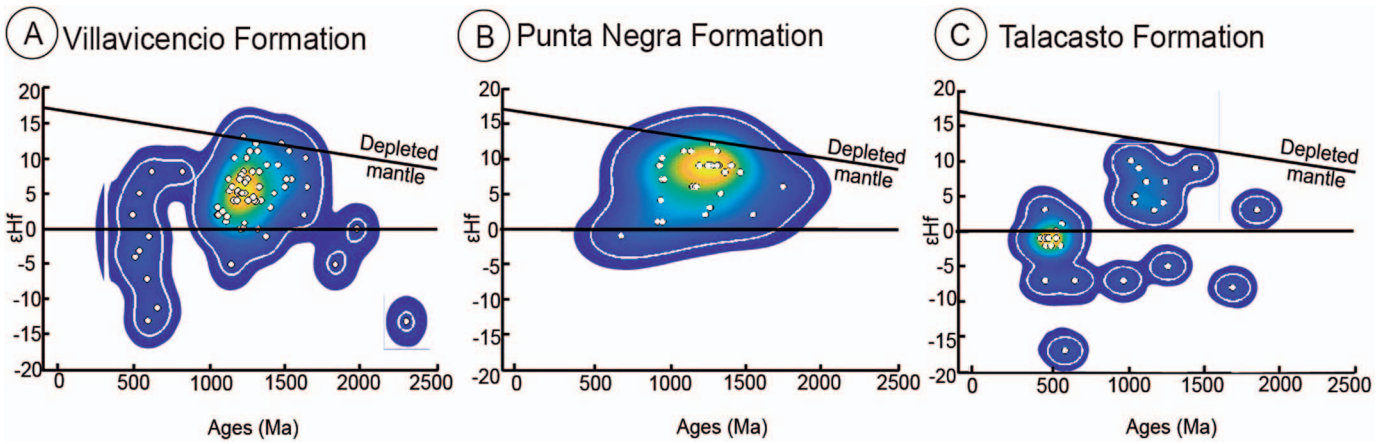

FIG. 12.—Kernel diagram showing the distribution and concentration of the U-Pb age (LA-ICP-MS) of zircons with their respective εHf. **A)** Villavicencio Fm. **B)** Punta Negra Fm. **C)** Talacasto Fm.

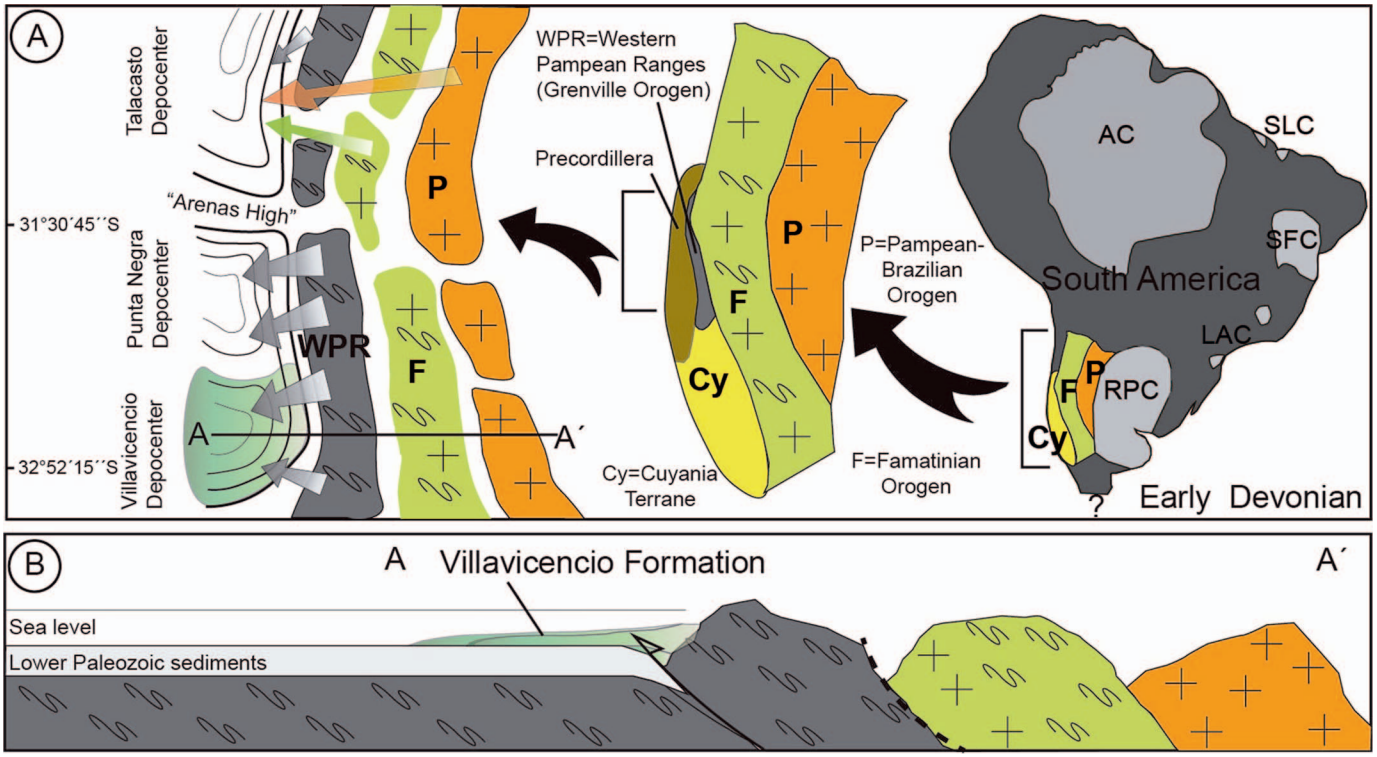

FIG. 13.—Schematic local geotectonic setting and the different contributing sources in the southwest margin of Gondwana. **A)** Location of cratons in South America (light gray, RPC, Rio de la Plata Craton; LAC, Luis Alves Craton; SFC, São Francisco Craton; SLC, São Luis Craton; AC, Amazonas Craton) and distribution of the main orogeny in central Argentina. Orange arrow, Pampean–Brazilian source. Green arrow, Famatinian source; gray arrow, Mesoproterozoic source. **B)** A–A′, simplified profile (modified and simplified from Arnol et al. 2020, 2022). Estimated coordinates are of the present time.

possibly forming a mountain range of greater continuity than the modern one. This mountain range, besides being the main source area, would have acted as a topographic barrier for the subordinate Famatinian and Pampean–Brazilian sources of the Villavicencio Formation. While to the north in the Central San Juan Precordillera (Arnol et al. 2022), a certain discontinuity of the chain would have allowed greater contributions of the Famatinian and Pampean–Brazilian orogens for the Talacasto Formation (Fig. 13).

FINAL REMARKS

- Petrographic and geochemical analyses point to null or slightly weathered very fine-grained sandstones and pelites, with low reworking, derived from igneous–metamorphic sources with an average composition similar to upper continental crust. Uranium gain of certain samples reinforces deposition by hyperpycnal flows in a deltaic environment.
- Derivation from an igneous–metamorphic basement, though not extensively reworked, is further supported by zircon internal textures and external morphologies.
- Lu-Hf data indicate that the main Mesoproterozoic source deduced by previous authors (most likely the Western Pampean Ranges) are characterized by juvenile-mantle signatures.
- Multiple independent provenance proxies reinforce the hypothesized equivalence between the Villavicencio Formation of the Mendoza Precordillera and the Punta Negra Formation of the Central San Juan Precordillera.
- The Western Pampean Ranges were uplifted before the Middle Devonian in order to provide detritus to the Villavicencio basin.

CREDIT AUTHORSHIP CONTRIBUTION STATEMENT

Federico D. Wenger: writing, original draft, methodology, investigation, formal analysis, conceptualization. Jonatan A. Arnol: writing, original draft, methodology, supervision, investigation. Norberto J. Uriz: field work, writing, review and editing, supervision, conceptualization. Carlos A. Cingolani: field work, writing, review and editing, supervision, conceptualization. Paulina Abre: writing, review and editing, supervision, conceptualization. Miguel A.S. Basei: supervision, methodology, formal analysis.

SUPPLEMENTAL MATERIAL

Supplemental material is available from the SEPM Data Archive: https://www.sepm.org/supplemental-materials.

ACKNOWLEDGMENTS

This research was partially financed by Consejo Nacional de Investigaciones Científicas y Técnicas (CONICET), Argentina (Grant PUE–CIG) and the University of La Plata, Argentina, project PIPD/N040. División Geología (La Plata Museum–UNLP), the Centro de Investigaciones Geológicas (CIG, La Plata, Argentina), and Centro de Pesquisas Geocronológicas (CPGeo, São Paulo, Brazil) provided laboratory facilities for sample preparation and analysis.

We heartily express our gratitude for the comments and suggestions of reviewers Tomas Capaldi, Kelly Thomson, and Associate Editor Andrea Fildani, who considerably improved the original manuscript.

REFERENCES

ABRE, P., CINGOLANI, C.A., ZIMMERMANN, U., CAIRNCROSS, B., AND CHEMALE, F., 2011, Provenance of Ordovician clastic sequences of the San Rafael Block (central Argentina),

with emphasis on the Ponón Trehué Formation: Gondwana Research, v. 19, p. 275–290, doi:10.1016/J.GR.2010.05.013.

Abre, P., Cingolani, C.A., Cairncross, B., and Chemale, F., 2012, Siliciclastic Ordovician to Silurian units of the Argentine Precordillera: constraints on provenance and tectonic setting in the proto-Andean margin of Gondwana: Journal of South American Earth Sciences, v. 40, p. 1–22, doi:10.1016/J.JSAMES.2012.07.013.

Abre, P., Cingolani, C.A., Chemale, F., and Uriz, N.J., 2017, La Horqueta Formation: geochemistry, isotopic data, and provenance analysis, *in* Cingolani, C., ed., Pre-Carboniferous Evolution of the San Rafael Block, Argentina: Springer Earth System Sciences, doi:10.1007/978-3-319-50153-6_9.

Anani, C., Asiedu, D.K., Atta-Peters, D., and Manu, J., 2012, Zircon typology as indicator of provenance in Neoproterozoic sandstones of the Voltaian Basin, Ghana: Journal of Environmental and Earth Sciences, v. 4, p. 151–161.

Arnol, J.A., and Coturel, E.P., 2022, Early Devonian paleogeographic evolution of SW Gondwana (Precordillera Argentina): How can the record of plants help us?: Journal of South American Earth Sciences, v. 114, no. 103680, doi:10.1016/j.jsames.2021.103680.

Arnol, J.A., Uriz, N.J., Cingolani, C.A., Basei, M.A.S., and Abre, P., 2020, Provenance analysis of Devonian peripheral foreland basins in SW Gondwana, case of the Gualilán Group, Precordillera Argentina: International Journal of Earth Sciences, v. 109, p. 2467–2494, doi:10.1007/s00531-020-01914-9.

Arnol, J.A., Uriz, N.J., Cingolani, C.A., Abre, P., and Basei, M.A.S., 2022, Provenance evolution of the San Juan Precordillera Silurian–Devonian basin (Argentina): linking with other depocentres in Cuyania terrane: Journal of South American Earth Sciences, v. 115, no. 103766, doi:10.1016/J.JSAMES.2022.103766.

Arnol, J.A., Cretacotta, A., Uriz, N.J., Cingolani, C.A., and Basei, M.A.S., 2023, New insights on the interpretation of the provenance and evolution of the Silurian units in the central Precordillera, Argentina: Journal of South American Earth Sciences, v. 124, no. 104245, doi:10.1016/j.jsames.2023.104245.

Astini, R.A., 1992, Tectofacies ordovícicas y evolución de la cuenca eopaleozoica de la precordillera Argentina: Estudios Geológicos, v. 48, p. 315–327, doi:10.3989/EGEOL.92485-6398.

Astini, R.A., Benedetto, J.L., and Vaccari, N.E., 1995, The early Paleozoic evolution of the Argentine Precordillera as a Laurentian rifted, drifted, and collided terrane: a geodynamic model: Geological Society of America, Bulletin, v. 107, p. 253–273.

Bahlburg, H., and Dobrzinski, N., 2011, A review of the Chemical Index of Alteration (CIA) and its application to the study of Neoproterozoic glacial deposits and climate transitions, *in* Arnaud, E., Halverson, G.P., and Shields-Zhou, G., eds., The Geological Record of Neoproterozoic Glaciations: Geological Society of London, Memoir 36, p. 81–92, doi:10.1144/M36.6.

Baldis, B.A., Uliarte E., and Vaca A., 1980, El frente estructural de la Precordillera mendocina: Boletín Museo de Ciencias Naturales y Antropológicas, Juan C. Moyano, v. 1, p. 6–12.

Barton, M., and Rodríguez, E., 1989, Geología del piedemonte de la Sierra de Uspallata al oeste de la ciudad de Mendoza: detección y control de la desertificación: II Curso Latinoamericano de Desertificación, p. 154–159.

Benedetto, J.L., 2004, The allochthony of the Argentine Precordillera ten years later (1993–2003): a new paleobiogeographic test of the microcontinental model: Gondwana Research, v. 7, p. 1027–1039, doi:10.1016/S1342-937X(05)71082-0.

Boedo, F.L., Pérez Luján, S., Naipauer, M., Vujovich, G.I., Pimentel, M.M., Ariza, J.P., and Barredo, S.P., 2020, The Late Neoproterozoic–Early Paleozoic basin of the western Argentine Precordillera: insights from zircon U-Pb geochronology: Journal of South American Earth Sciences, v. 102, no. 102669, doi:10.1016/J.JSAMES.2020.102669.

Borrello, A.V., 1969, Los Geosinclinales de la Argentina: Buenos Aires, Dirección Nacional de Geología y Minería, v. 14, p. 1–188.

Bracaccini, O.I., 1949, El perfil de Tambolar (provincia de San Juan): Revista de La Asociación Geológica Argentina, v. 4, p. 165–179.

Bracaccini, O.I., 1964, Geología estructural de la zona cordillerana de Mendoza y Neuquén, República Argentina: Buenos Aires, Dirección General de Fabricaciones Militares, v. 14, no. 1103.

Bustos U.D., 1995, Sedimentología y evolución paleoambiental de la Formación Punta Negra en el sector central de la Precordillera de San Juan [BA Thesis]: Facultad de Ciencias Exactas, Fisicas y Naturales, Universidad Nacional de Córdoba, 120 p.

Cingolani, C.A., Manassero, M., Basei, M., and Uriz, N.J., 2013, Provenance of the Villavicencio Formation (Lower Devonian) in the southern sector of the Precordillera, Mendoza, Argentina: new sedimentary and geochronological data: Montevideo, I Congreso de Minería y Geología Del Cono Sur, Proceedings, v. I, p. 191–196.

Cingolani, C.A., Uriz, N.J., Abre, P., Manassero, M.J., and Basei, M.A.S., 2017, Silurian–Devonian land–sea interaction within the San Rafael Block, Argentina: provenance of the Río Seco de los Castaños Formation, *in* Cingolani, C., ed., Pre-Carboniferous Evolution of the San Rafael Block, Argentina: Springer Earth System Sciences, doi:10.1007/978-3-319-50153-610.

Cristallini, E.O., and Ramos, V.A., 2000, Thick-skinned and thin-skinned thrusting in the La Ramada fold and thrust belt: crustal evolution of the High Andes of San Juan, Argentina (32 SL): Tectonophysics, v. 317, p. 205–235.

Cuerda, A.J., 1988, Investigaciones estratigráficas en el Grupo Villavicencio, precordillera de Mendoza y San Juan, R. Argentina: V Congreso Geológico Chileno 39, p. 177–187.

Cuerda, A.J., and Baldis, B.A., 1971, Silúrico–Devónico de la Argentina: Ameghiniana, v. 8, p. 127–164.

Cuerda, A., Cingolani, C.A., Arrondo, O., Morel, E., and Ganuza, D., 1987, Primer registro de plantas vasculares en la Formación Villavicencio, Precordillera de Mendoza, Argentina: IV Congreso Latinoamericano de Paleontología, p. 179–183.

Cuerda, A.J., Cingolani, C.A., Bordonaro, O., and Ramos, V.A., 1993, Las secuencias sedimentarias eopaleozoicas, Geología y Recursos Naturales de Mendoza: Congreso Geológico Argentino and Congreso de Exploración de Hidrocarburos, Proceedings, v. 1, p. 21–30.

Cullers, R.L., 1995, The controls on the major- and trace-element evolution of shales, siltstones, and sandstones of Ordovician to Tertiary age in the Wet Mountains region, Colorado, USA: Chemical Geology, v. 123, p. 107–131.

Dalla Salda, L., Cingolani, C.A., and Varela, R., 1992, Early Paleozoic orogenic belt of the Andes in southwestern South America: result of Laurentia–Gondwana collision?: Geology, v. 20, p. 617–620.

Dalziel, I.W.D., 1997, Overview: Neoproterozoic–Paleozoic geography and tectonics: review, hypothesis, environmental speculation: Geological Society of America, Bulletin, v. 109, p. 16–42.

Dalziel, I.W.D., Dalla Salda, L.H., and Gahagan, L.M., 1994, Paleozoic Laurentia–Gondwana interaction and the origin of the Appalachian–Andean Mountain system: Geological Society of America, Bulletin, v. 106, p. 243–252.

Daneshvar, N., Maanijou, M., Azizi, H., and Asahara, Y., 2018, Study of the zircon morphology and internal structures as a tool for constraining magma source: example from granitoid bodies in the northern Sanandaj Sirjan zone (SW Saqqez): Geopersia, v. 8, p. 245–259.

Dickinson, W.R., and Gehrels, G.E., 2003, U-Pb ages of detrital zircons from Permian and Jurassic eolian sandstones of the Colorado Plateau, USA: paleogeographic implications: Sedimentary Geology, v. 163, p. 29–66, doi:10.1016/S0037-0738(03)00158-1.

Dickinson, W.R., Beard, L.S., Brakenridge, G.R., Erjavec, J.L., Ferguson, R.C., Inman, K.F., Knepp, R.A., Lindberg, F.A., and Ryberg, P.T., 1983, Provenance of North American Phanerozoic sandstones in relation to tectonic setting: Geological Society of America, Bulletin, v. 94, p. 222–235.

Dypvik, H., and Harris, N.B., 2001, Geochemical facies analysis of fine–grained siliciclastics using Th/U, Zr/Rb and (Zr+Rb)/Sr ratios: Chemical Geology, v. 181, p. 131–146, doi:10.1016/S0009-2541(01)00278-9.

Edwards, D., Morel, E., Poiré, D.G., and Cingolani, C.A., 2001, Land plants in the Devonian Villavicencio Formation, Mendoza Province, Argentina: Review of Palaeobotany and Palynology, v. 116, p. 1–18, doi:10.1016/S0034-6667(01)00059-8.

Edwards, D., Poiré, D.G., Morel, E.M., and Cingolani, C.A., 2009, Plant assemblages from SW Gondwana: further evidence for high-latitude vegetation in the Devonian of Argentina, *in* Bassett, M.G., ed., Early Palaeozoic peri-Gondwana terranes: new insights from tectonics and biogeography: Geological Society of London, Special Publication, 325, p. 233–255.

Fedo, C.M., Sircombe, K.N., and Rainbird, R.H., 2003, Detrital zircon analysis of the sedimentary record: Reviews in Mineralogy and Geochemistry, v. 53, p. 277–303, doi:10.2113/0530277.

Finney, S.C., 2007, The parautochthonous Gondwanan origin of the Cuyania (greater Precordillera) terrane of Argentina: a re-evaluation of evidence used to support an allochthonous Laurentian origin: Geologica Acta, v. 5, p. 127–158, doi:10.1344/105.000000300.

Floyd, P.A., and Leveridge, B.E., 1987, Tectonic environment of the Devonian Gramscatho basin, south Cornwall: framework mode and geochemical evidence from turbiditic sandstones (England): Geological Society of London, v. 144, p. 531–542, doi:10.1144/GSJGS.144.4.0531.

Galindo, C., Casquet, C., Rapela, C.W., Pankhurst, R.J., Baldo, E., and Saavedra, J., 2004, Sr, C, and O isotope geochemistry and stratigraphy of Precambrian and lower Paleozoic carbonate sequences from the western Sierras Pampeanas of Argentina: tectonic implications: Precambrian Research, v. 131, p. 55–71.

Gärtner, A., Linnemann, U., Sagawe, A., Hofmann, M., Ullrich, B., and Kleber, A, 2013, Morphology of zircon crystal grains in sediments: characteristics, classifications, definitions: Journal of Central European Geology, v. 59, p. 65–73.

Garzanti, E., 2016, From static to dynamic provenance analysis: sedimentary petrology upgraded: Sedimentary Geology, v. 336, p. 3–13, doi:10.1016/j.sedgeo.2015.07.010.

Garzanti, E., 2019, Petrographic classification of sand and sandstone: Earth-Science Reviews, v. 192, p. 545–563, doi:10.1016/j.earscirev.2018.12.014.

Giambiagi, L., Mescua, J., Folguera, A., and Martínez, A., 2010, Estructuras y cinemática de las deformaciones pre-Andinas del sector sur de la precordillera, Mendoza: Revista Asociación Geológica Argentina, v. 66, p. 5–20.

Harrington, H.J., 1941, Investigaciones geológicas en las Sierras de Villavicencio y Mal País, Provincia de Mendoza: Dirección de Minas y Geología, v. 49, p. 1–55.

Harrington, H.J., 1957, Ordovician formations of Argentina, *in* Harrington, H.J., and Leanza, A.F., Ordovician trilobites of Argentina: Department of Geology, University of Kansas, Lawrence, Special Publication 1, p. 1–59.

Harrington, H.J., 1971, Descripción Geológica de la Hoja 22 c, Ramblón, Provincias de Mendoza y San Juan, Carta Geológico-Económica de la República Argentina, scale 1:200,000.

Heaman, L.M., Bowins, R., and Crocket, J., 1990, The chemical composition of igneous zircon suites: implications for geochemical tracer studies: Geochimica et Cosmochimica Acta, v. 54, p. 1597–1607, doi:10.1016/0016-7037(90)90394-Z.

Heredia, S., 1990, Geología de la Cuchilla del cerro Pelado, Precordillera de Mendoza, Argentina: San Juan, XI Congreso Geológico Argentino, Proceedings, v. 2, p. 101–104.

Hessler, A.M., and Fildani, A., 2019, Deep-sea fans: tapping into Earth's changing landscapes: Journal of Sedimentary Research, v. 89, p. 1171–1179, doi:2019112712503258100.

Hiscott, R.N., 1984, Ophiolitic source rocks for Taconic-age flysch: trace-element evidence: Geological Society of America, Bulletin, v. 95, p. 1261–1267.

Ingersoll, R., Bullard, T.F., Ford, R.L., Grimm, J.P., Pickle, J.D., and Sares, S.W., 1984, The effect of grain size on detrital modes: a test of the Gazzi-Dickinson point-counting method: Journal of Sedimentary Petrology, v. 54, p. 103–116, doi:10.1306/212F83B9-2B24-11D7-8648000102C1865D.

Jordán, T.E., Isacks, B.L., Allmendinger, R.W., Brewer, J.A., Ramos, V.A., and Ando, C.J., 1983, Andean tectonics related to geometry of subducted Nazca Plate: Geological Society of America, Bulletin, v. 94, p. 341–361.

Keller, M., 1999, Argentine Precordillera: sedimentary and plate tectonic history of a Laurentian crustal fragment in South America, *in* Keller, M., ed., Argentine Precordillera: Sedimentary and Plate Tectonic History of a Laurentian Crustal Fragment in South America: Geological Society of America, Special Publication 341, 131 p.

Kury, W., 1993, Características composicionales de la Formación Villavicencio, Devónico, Precordillera de Mendoza: XII Congreso Geológico Argentino y II Congreso de Exploración de Hidrocarburos, Geología y Recursos Naturales de Mendoza, Proceedings, v. 1, p. 321–328.

Kury, W., 1994, Sedimentologische Untersuchung der Formation Villavicencio Präkordillere von Mendoza Argentinien: Fakultät für Geowissenschaften, Ludwig Maximilians Universität.

Liu, Y., Hu, Z., Zong, K., Gao, C., Gao, S., Xu, J., and Chen, H., 2010, Reappraisement and refinement of zircon U–Pb isotope and trace element analyses by LA-ICP-MS: Chinese Science Bulletin, v. 55, p. 1535–1546.

Loske, W.P., 1992, Sedimentologie, Herkunft und geotektonische Entwicklung paläozoischer Gesteine der Präkordillere West-Argentiniens: Institut für Allgemeine und Angewandte Geologie, Ludwig Maximilians Universität München.

Loske, W.P., 1994, The West-Argentine precordillera: a Palaeozoic back arc basin: Zeitschrift Der Deutsche Geologische Gesellschaft, v. 145, p. 379–391, doi:10.1127/ZDGG/145/1994/379.

Loske, W.P., 1995, 1.1 Ga old zircons in W Argentina: implications for sedimentary provenance in the Palaeozoic of Western Gondwana: Neues Jahrbuch für Geologie und Paläontologie, Monatshefte, v. 1995, p. 51–64, doi:10.1127/NJGPM/1995/1995/51.

Malusà, M.G., Carter, A., Limoncelli, M., Villa, I.M., and Garzanti, E., 2013, Bias in detrital zircon geochronology and thermochronometry: Chemical Geology, v. 359, p. 90–107, doi:10.1016/j.chemgeo.2013.09.016.

Manassero, M.J., Cingolani, C.A., and Abre, P., 2009, A Silurian–Devonian marine platform–deltaic system in the San Rafael Block, Argentine Precordillera–Cuyania terrane: lithofacies and provenance, *in* Könighshof, P., ed., Devonian change: case studies in palaeogeography and palaeoecology: The Geological Society of London, Special Publication, v. 314, p. 215–240, doi:10.1144/SP314.12.

Martin, E.L., Collins, W.J., and Spencer, C.J., 2020, Laurentian origin of the Cuyania suspect terrane, western Argentina, confirmed by Hf isotopes in zircon: Geological Society of America, Bulletin, v. 132, p. 273–290, doi:10.1130/B35150.1.

McLennan, S., 1989, Rare earth elements in sedimentary rocks: influence of provenance and sedimentary processes, *in* Lipin, B., and McKay, G., eds., Geochemistry and Mineralogy of Rare Earth Elements: De Gruyter, p. 169–200, doi:10.1515/9781501509032-010.

McLennan, S.M., Hemming, S., McDaniel, D.K., and Hanson, G.N., 1993, Geochemical approaches to sedimentation, provenance, and tectonics, *in* Johnsson, M.J., and Basu, A., eds., Processes Controlling the Composition of Clastic Sediments: Geological Society of America, Special Publication 21, p. 21.

McLennan, S.M., Grotzinger, J.P., Hurowitz, J.A., and Tosca, N.J., 2006, Sulfate Geochemistry and the Sedimentary Rock Record of Mars: Workshop on Martian Sulfates as Records of Atmospheric–Fluid–Rock Interactions: Houston, The Lunar and Planetary Institute, no. 1331, p. 54.

Mouro, L.D., Rakociński, M., Marynowski, L., Pisarzowska, A., Musabelliu, S., Zatoń, M., Carvalho, M.A., Fernandes, A.C.S., and Waichel, B.L., 2017, Benthic anoxia, intermittent photic zone euxinia and elevated productivity during deposition of the Lower Permian, post-glacial fossiliferous black shales of the Paraná Basin, Brazil: Global and Planetary Change, v. 158, p. 155–172, doi:10.1016/J.GLOPLACHA.2017.09.017.

Naipauer, M., Vujovich, G.I., Cingolani, C.A., and McClelland, W.C., 2010, Detrital zircon analysis from the Neoproterozoic–Cambrian sedimentary cover (Cuyania terrane), Sierra de Pie de Palo, Argentina: evidence of a rift and passive margin system?: Journal of South American Earth Sciences, v. 29, p. 306–326, doi:10.1016/J.JSAMES.2009.10.001.

Nance, W.B., and Taylor, S.R., 1976, Rare earth element patterns and crustal evolution, I. Australian post-Archean sedimentary rocks: Geochimica et Cosmochimica Acta, v. 40, p. 1539–1551.

Nesbitt, H.W., and Young, G.M., 1982, Early Proterozoic climates and plate motions inferred from major element chemistry of lutites, II: Nature, v. 299, p. 715–717.

Nesbitt, H.W., and Young, G.M., 1984, Prediction of some weathering trends of plutonic and volcanic rocks based on thermodynamic and kinetic considerations: Geochimica et Cosmochimica Acta, v. 48, p. 1523–1534, doi:10.1016/0016-7037(84)90408-3.

Nesbitt, H.W., and Young, G.M., 1989, Formation and diagenesis of weathering profiles: Journal of Geology, v. 97, p. 129–147.

Ortiz, A., and Zambrano, J.J., 1981, La provincia geológica Precordillera oriental: VIII Congreso Geológico Argentino, v. 3, p. 59–74.

Padula, E.L., Rolleri, E.O., Mingramm, A.R.G., Roque, P.C., Flores, M.A., and Baldis, B.A., 1967, Devonian of Argentina, *in* Oswald, D.H., ed., International Symposium on the Devonian System: Canadian Society of Petroleum Geologists, Special Publication 2, p. 165–199.

Poiré, D., and Morel, E., 1996, Procesos sedimentarios vinculados a la depositación de niveles con plantas en secuencias Siluro–Devónicas de la Precordillera, Argentina: VI Reunión Argentina de Sedimentología, Proceedings, v. 1, p. 205–210.

Poiré, D.G., Edwards, D., Morel, E., Bassett, M.G., and Cingolani, C.A., 2005, Depositional environments of Devonian land plants from Argentine Precordillera, South-West Gondwana [Abstract]: Mendoza, Gondwana 12 Conference.

Pupin, J.P., 1980, Zircon and granite petrology: Contributions to Mineralogy and Petrology, v. 73, p. 207–220, doi:10.1007/BF00381441.

Ragona, D., Anselmi, G., González, P., and Vujovich, G., 1995, Mapa Geológico de la Provincia de San Juan: República Argentinas, scale 1:500,000.

Rakociński, M., Pisarzowska, A., Janiszewska, K., and Szrek, P., 2016, Depositional conditions during the Lower Kellwasser Event (Late Frasnian) in the deep-shelf Łysogóry Basin of the Holy Cross Mountains Poland: Lethaia, v. 49, p. 571–590, doi:10.1111/LET.12167.

Ramacciotti, C.D., Baldo, E.G., and Casquet, C., 2015, U-Pb SHRIMP detrital zircon ages from the Neoproterozoic Difunta Correa metasedimentary sequence (Western Sierras Pampeanas, Argentina): provenance and paleogeographic implications: Precambrian Research, v. 270, p. 39–49, doi:10.1016/J.PRECAMRES.2015.09.008.

Ramos, V.A., Jordan, T.E., Allmendinger, R.W., Mpodozis, C., Kay, S.M., Cortes, J.M., and Palma, M., 1986, Paleozoic terranes of the central Argentine–Chilean Andes: Tectonics, v. 5, p. 855–880, doi:10.1029/TC005i006p00855.

Ramos, V.A., Cristallini, E.O., and Pérez, D.J., 2002, The Pampean flat-slab of the Central Andes: Journal of South American Earth Sciences, v. 15, p. 59–78.

Rapela, C.W., Pankhurst, R.J., Casquet, C., Baldo, E., Galindo, C., Fanning, C.M., and Dahlquist, J.M., 2010, The Western Sierras Pampeanas: protracted Grenville-age history (1330–1030 Ma) of intra-oceanic arcs, subduction-accretion at continental-edge and AMCG intraplate magmatism: Journal of South American Earth Sciences, v. 29, p. 105–127, doi:10.1016/J.JSAMES.2009.08.004.

Rapela, C.W., Verdecchia, S.O., Casquet, C., Pankhurst, R.J., Baldo, E.G., Galindo, C., Murra, J.A., Dahlquist, J.A., and Fanning, M.C., 2016, Identifying Laurentian and SW Gondwana sources in the Neoproterozoic to early Paleozoic metasedimentary rocks of the Sierras Pampeanas: paleogeographic and tectonic implications: Gondwana Research, v. 32, p. 193–212.

Rubinstein, C., 1993, Nota Paleontológica, primer registro de miosporas y acritarcos del Devónico Inferior, en el "Grupo Villavecencio," Precordillera de Mendoza, Argentina: Ameghiniana, v. 30, p. 219–220.

Rubinstein, C., and Steemans, P., 2007, New palynological data from the Devonian Villavicencio Formation, Precordillera of Mendoza, Argentina: Ameghiniana, v. 44, p. 3–9.

Satellite image, no date, Google, sampling area, Fig. 4A, Retrieved 1/2014, from https://shorturl.at/dFGN2.

Satellite image, no date, Google, sampling area, Fig. 4B, Retrieved 1/2014, from https://shorturl.at/antwy.

Satellite image, no date, Google, sampling area, Fig. 4C, Retrieved 1/2014, from https://shorturl.at/kwCHX.

Sun, S.S., and McDonough, W.F., 1989, Chemical and isotopic systematics of oceanic basalts: implications for mantle composition and processes, *in* Saunders, A.D., and Norry, M.J., eds., Magmatism in Ocean Basins: Geological Society of London, Special Publication 42, p. 313–345, doi:10.1144/GSL.SP.1989.042.01.19.

Taylor, S.R., and McLennan, S.M., 1985, The continental crust: its composition and evolution: Journal of Geology, v. 97, p. 735–747, doi:10.1086/629355.

Thomas, W.A., and Astini, R.A., 1996, The Argentine precordillera: a traveler from the Ouachita embayment of North American Laurentia: Science, v. 273, p. 752–757.

Thomas, W.A., Astini, R.A., Mueller, P.A., and McClelland, W.C., 2015, Detrital–zircon geochronology and provenance of the Ocloyic synorogenic clastic wedge, and Ordovician accretion of the Argentine Precordillera terrane: Geosphere, v. 11, p. 1749–1769, doi:10.1130/GES01212.1.

Uriz, N.J., Cingolani, C.A., Taboada, A.C., Arnol, J.A., Basei, M.A.S., Abre, P., and Coelho dos Santos, G.S., 2022, Provenance of pre- and Carboniferous sequences of the Esquel–Arroyo Pescado–Tepuel regions (Argentine Patagonia): a combined U–Pb and Hf isotope study of detrital zircon and constraints on depositional setting: Journal of South American Earth Sciences, v. 119, no. 103953, doi:10.1016/J.JSAMES.2022.103953.

Varela, R., Basei, M.A.S., González, P.D., Sato, A.M., Naipauer, M., Neto, M.C., Cingolani, C.A., and Meira, V.T., 2011, Accretion of Grenvillian terranes to the southwestern border of the Río de la Plata craton, western Argentina: International Journal of Earth Sciences, v. 100, p. 243–272, doi:10.1007/S00531-010-0614-2/FIGURES/10.

Waisfeld, B.G., Benedetto, J.L., Toro, B.A., Voldman, G.G., Rubinstein, C.V., Heredia, S., Assine, M.L., Vaccari, N.E., and Niemeyer, H., 2023, The Ordovician of southern South America, *in* Servais, T., Harper, D.A.T., Lefebvre, B., and Percival, I.G., eds., A Global Synthesis of the Ordovician System: Part 2: Geological Society of London, Special Publication 533, 42 p. doi:10.1144/SP533-2022-95.

Watson, E.B., 1996, Surface enrichment and trace-element uptake during crystal growth: Geochimica et Cosmochimica Acta, v. 60, p. 5013–5020, doi:10.1016/S0016-7037(96)00299-2.

Watson, E.B., and Liang, Y., 1995, A simple model for sector zoning in slowly grown crystals: implications for growth rate and lattice diffusion, with emphasis on accessory minerals in crustal rocks: American Mineralogist, v. 80, p. 1179–1187, doi:10.2138/AM-1995-11-1209.

Woodhead, J.D., and Hergt, J.M., 2005, A preliminary appraisal of seven natural zircon reference materials for in situ Hf isotope determination: Geostandards and Geoanalytical Research, v. 29, p. 183–195.

Yang, J.H., Wu, F.Y., Wilde, S.A., Xie, L.W., Yang, Y.H., and Liu, X.M., 2007, Tracing magma mixing in granite genesis: in situ U-Pb dating and Hf-isotope analysis of zircons: Contributions to Mineralogy and Petrology, v. 153, p. 177–190.

Zavala, C., Arcuri, M., Di Meglio, M., Zorzano, A., Otharán, G., Irastorza, A., and Torresi, A., 2021, Deltas: a new classification expanding Bates's concepts: Journal of Palaeogeography, v. 10, p. 1–15, doi:10.1186/s42501-021-00098-w.

Received 1 December 2022; accepted 29 May 2023.